Supporting Information

Precise Tuning of Cationic Cyclophanes toward Highly Selective Fluorogenic Recognition of Specific Biophosphate Anions

Muhammad Yousuf,[†,§] Nisar Ahmed,*[,‡] Bahareh Shirinfar,[‡] Vijay Madhav Miriyala,[†] Il Seung Youn,[†,§] and Kwang S. Kim*[,§]

[†]Department of Chemistry, Pohang University of Science and Technology, Pohang 790-784, Korea
[‡]Organic Chemistry Institute, University of Zürich (UZH) Winterthurerstrasse 190, 8057 Zürich (Switzerland)
[§]Department of Chemistry, Ulsan National Institute of Science and Technology (UNIST), Ulsan 689-798, Korea

Ulsan University of Science and Technology
Ulsan 689-798, Korea
Phone : + 82-52-217-5410, Fax: +82-52-217-5419
Email: kimks@unist.ac.kr (ksk), nisar.ahmed@chem.uzh.ch (na)*

Experimental techniques:

General consideration:

New cyclophanes were fully characterized with standard spectroscopic techniques. Microanalyses were performed on a Carlo 1102 elemental analysis instrument. Electronic absorption (UV-Vis) spectra were recorded using a Shanghi 756 MC UV-Vis spectrometer. ^{1}H NMR, ^{13}C NMR, HSQC, COSY and NOESY spectra were performed on a Bruker Advance DPX500 (500 and 600 MHz) and Varian VNMRS 600 spectrometer at 298 K. High resolution mass spectra were obtained on a Micromass Platform II mass spectrometer. Fluorescence studies were carried out on Shimadzu RF-5301 PC spectrofluorophotometer at 298 K. Imidazole, 2,6-Bis(bromomethyl)naphthalene, acridine, bromomethyl methylether (BMME), benzaldehyde, di(imidazol-1-yl)methanone and cobalt chloride hexahydrate ($CoCl_2.6H_2O$) were purchased from Aldrich, while 9,10-bis(bromomethyl) anthracene was purcghased from Santa Crutz laboratories and were used as such. Sodium salts of AMP, ADP, ATP, GMP, GDP, GTP, CMP, CTP, TMP, TTP, UMP, UTP and *n*-TBA salts of F^-, Cl^-, I^-, $H_2PO_4^-$, $HP_2O_7^{3-}$, CH_3COO^- and NO_3^- were also purchased from Aldrich and used without further purification.

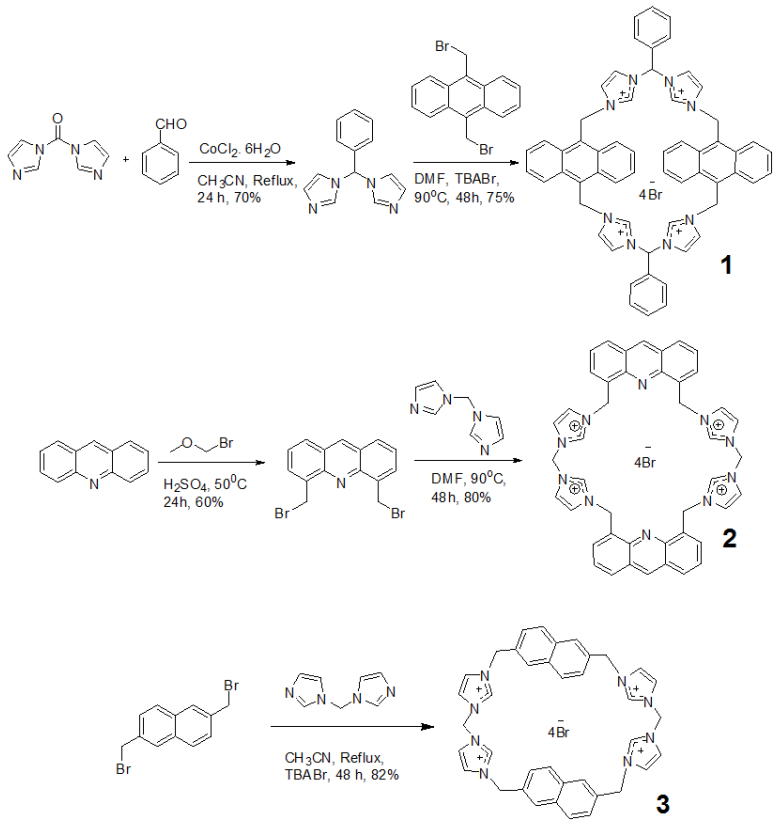

Scheme S1. Synthesis of cyclophanes **1**, **2** and **3.**

Synthesis of 1,1'-(phenylmethylene)bis(1*H*-imidazole) and Probe (1)

Synthesis of 1,1'-(phenylmethylene)bis(1*H*-imidazole):

To a stirred solution of benzaldehyde (2.3 ml, 21.75 mmol) and di(i-midazol-1-yl)methanone (3.5 g, 21.75 mmol) in dry CH_3CN (20 ml) was added cobalt chloride ($CoCl_2.6H_2O$, 40 mg, 0.2 mmol) as a catalyst at room temperature under N_2 atmosphere. The mixture was heated at reflux temperature for 8 h and then solution was filtered. The solvent was removed on rotary evaporator and the resulting solid was purified by column chromatography using $CHCl_3$/MeOH (99:1) to yield 1,1'-(phenylmethylene)bis(1H-imidazole) (**a**) (2 g, 70% yield) as light yellow solid. (M. P. 123^{o}C); ^{1}H NMR (600MHz, $(CD_3)_2SO$, 25^{o}C): δ 8.05 (s, 1H), 7.91 (s, 2H), 7.38–7.45 (m, 5H) and 7.00–7.03 ppm (m, 4H); ^{13}C NMR (125MHz, $(CD_3)_2SO$, 25^{o}C): δ 68.48, 118.64, 126.41, 129.08, 129.31, 129.54, 136.48 and 137.28 ppm. MS (FAB, m/z): $[M]^+$ calcd for $C_{13}H_{12}N_4$: 224.11; found: 224.11.

Synthesis of Probe (**1**)

A solution of 1,1'-(phenylmethylene)bis(1*H*-imidazole) (0.54 mmol, 121 mg), tetrabutyl ammonium bromide (0.54 mmol, 174 mg), and 9,10-bis(bromomethyl) anthracene (0.54 mmol, 197 mg) in dry DMF (10 mL) was stirred at 90°C for 48 hr under N_2 atmosphere. The resultant hot solution was filtered to collect light yellow precipitates. The precipitates were washed with DMF and acetone. Residue so obtained was recrystallized from CH_3OH. The obtained product was in 75% yield. (M. P. >300^{o}C dec.); ^{1}H NMR (600 MHz, $(CD_3)_2SO$, 25ºC) δ 6.66 (s, 8H, -N-C**H2**-C-), 7.40 (d, 4H, -N-C**H**=C**H**-N-), 7.55−7.75 (m, 18H, phenyl ring and anthracene ring), 8.11 (s, 4H, -N-C**H**=C**H**-N-), 9.66 (s, 10H, bridging benzyl and anthracene ring), 9.75 (s, 4H, imidazolium C2 H); ^{13}C NMR (125 MHz, $(CD_3)_2SO$, 25ºC) δ 45.36, 71.51, 121.07, 123.57, 124.84, 126.29, 127.58, 127.78, 129.55, 130.60, 130.89, 131.01, 138.00: Anal. Calcd for $C_{58}H_{48}Br_4N_8$: C, 51.49; H, 3.73; N, 13.65, Found: C, 50.5; H, 3.9; N, 13.51. MS(FAB, m/z): $[M-Br]^+$ calc.: 1097.16; found: 1097.16.

Synthesis of 4,5-bis(bromomethyl) acridine and Probe (2)

Synthesis of 4,5-bis(bromomethyl) acridine:

BMME (2.78 g, 22.32 mmol) was added dropwise to a solution of acridine (1 g, 5.58 mmol) in H_2SO_4 (10 mL) at 50^{o}C. The mixture was stirred at 50^{o}C under nitrogen environment for 24 hr. This mixture was poured in a vessel containing ice, and the resulting precipitates were filtered out. The filtered cake was dissolved in $CHCl_3$ and the organic phase was washed with water. Organic layer was then dried over anhydrous $MgSO_4$ and evaporated under vacuum. The residual product was further purified by silica gel chromatography (chloroform:hexane = 8:2) and a pale yellow solid was obtained. The solid was recrystallized by $CHCl_3$ to obtain yellowish green crystals (1.40 g, yield 60%). ^{1}H NMR ($CDCl_3$, 600 MHz, 25^{o}C): δ 5.41 (s, 4H, -C-C**H2**-Br), 7.48 (m, 2H), 7.91-7.97 (m, 4H), 8.75

(s, 1H, H-9); ^{13}C NMR ($CDCl_3$, 125 MHz, 25^{o}C): δ 30.40, 126.03, 127, 129.25, 131.32, 136.67, 136.69, 145.95: Anal. Calc. ($C_{15}H_{11}Br_2N$): C, 49.35; H, 3.04; N, 3.84. Found: C, 49.49; H, 3.03; N, 3.83.; MS (FAB, m/z): $[M]^+$ calc.: 364.92; found: 364.92.

Synthesis of Probe (**2**)

A solution of 1-(1H-imidazol-1-ylmethyl)-1*H*-imidazole (0.54 mmol, 148.2 mg) and 4,5-bis(bromomethyl) ancridine (0.54 mmol, 197 mg) in dry DMF (10 mL) was stirred at 90°C for 48 hr. The resultant hot solution was filtered to collect light yellow precipitates. The precipitates were washed with DMF and acetone. The residue so obtained was recrystallized from CH_3OH. The obtained product was in 80% yield. (M. P. >300ºC dec.); ^{1}H NMR (500 MHz, $(CD_3)_2SO$, 25ºC) δ 6.647 (s, 8H, -N-C**H2**-C-), 7.370 (s, 4H, -N-C**H2**-N-), 7.705−8.28 (m, 20H, imidazolium ring -N-C**H**=C**H**-N- and acridine ring), 9.309 (s, 2H, H-9 acridine), 9.709 (s, 4H, imidazolium C2 H); ^{13}C NMR (125 MHz, $(CD_3)_2SO$, 25ºC) δ 49.96, 58.37, 122.21, 122.53, 123.17, 126.01, 126.26, 129.81, 130.94, 131.98, 138.09, 138.47, 147.18.; Anal. Calcd for $C_{44}H_{38}Br_4N_{10}$: C, 51.49; H, 3.73; N, 13.65, Found: C, 51.5; H, 3.8; N, 13.55.; MS (FAB, m/z): $[M\text{-}Br]^+$ calc.: 947.09; found: 947.09.

Synthesis of Probe (3)

To a solution of 1-(1H-imidazol-1-ylmethyl)-1*H*-imidazole (0.54 mmol, 80mg) and tetrabutylammonium bromide (0.54 mmol, 174mg) in dry CH_3CN (10 mL) 2,6-bis(bromomethyl) naphthalene (0.54 mmol, 170mg) was added slowly then solution was heated under reflux at 80^{o}C for 24 h. The resulting hot solution was filtered and residue was washed with first with CH_3CN (20 mL) and then with methanol (20 mL). The product was dried under vacuum. The obtained product was in 82 % yield. (M. P. >300^{o}C dec.); ^{1}H NMR (600 MHz, $(CD_3)_2SO$, 25^o C) δ 5.62 (s, 8H, -N-CH2-C-), 6.67 (s, 4H, -N-CH2-N-), 7.59 (m, 4H, naphthalene ring), 7.81-8.05(m, 16H, -N-CH=CH-N- and naphthalene ring), 9.63 (S, 4H, imidazolium C2 H); ^{13}CNMR (500 MHz, $(CD_3)_2SO$, 25^{o}C) δ 52.85, 59.00, 122.96, 123.61, 127.03, 128.25, 129.41, 132.69, 132.91, 138.26.: Anal. Calcd. for $C_{38}H_{36}Br_4N_8$: C, 49.38; H, 3.93; N, 12.12, Found: C, 49.23; H, 4.03; N, 12.21.; MS (FAB, m/z): [M- Br]+ calc.: 845.06; found: 845.06

NMR spectral analysis:

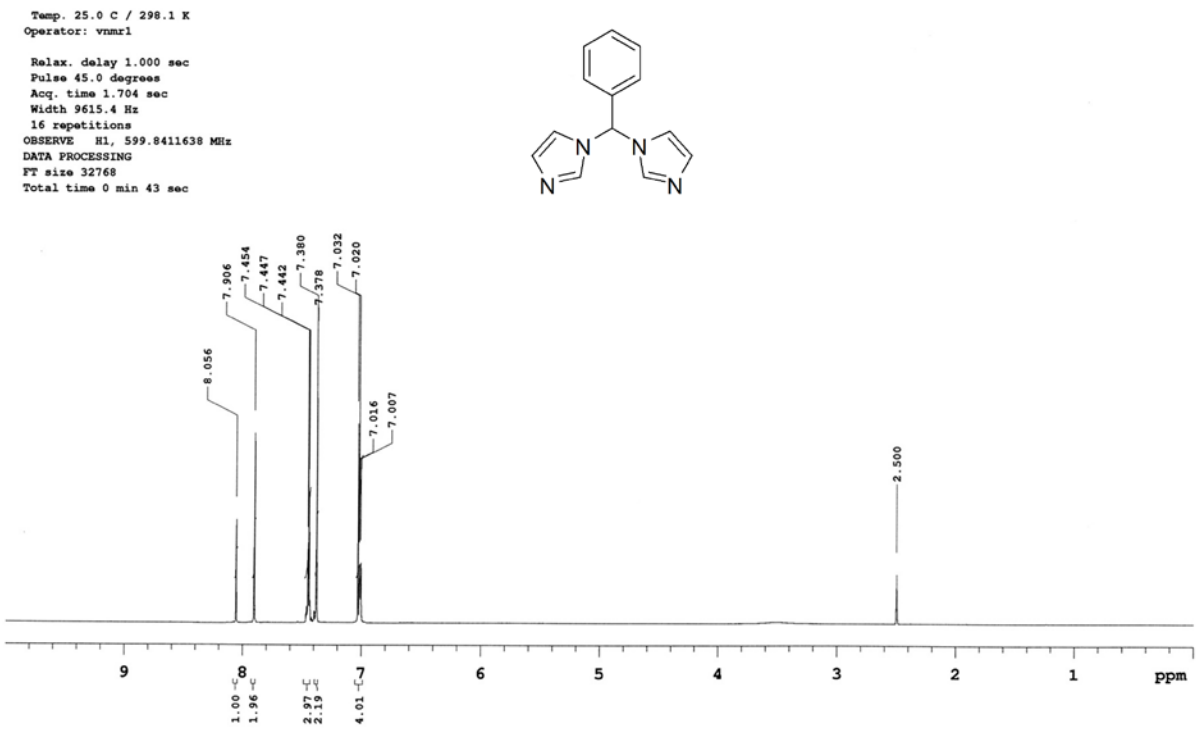

Figure S1. [1]H NMR spectrum of compound 1,1'-(phenylmethylene)bis(1H-imidazole) in DMSO-d_6.

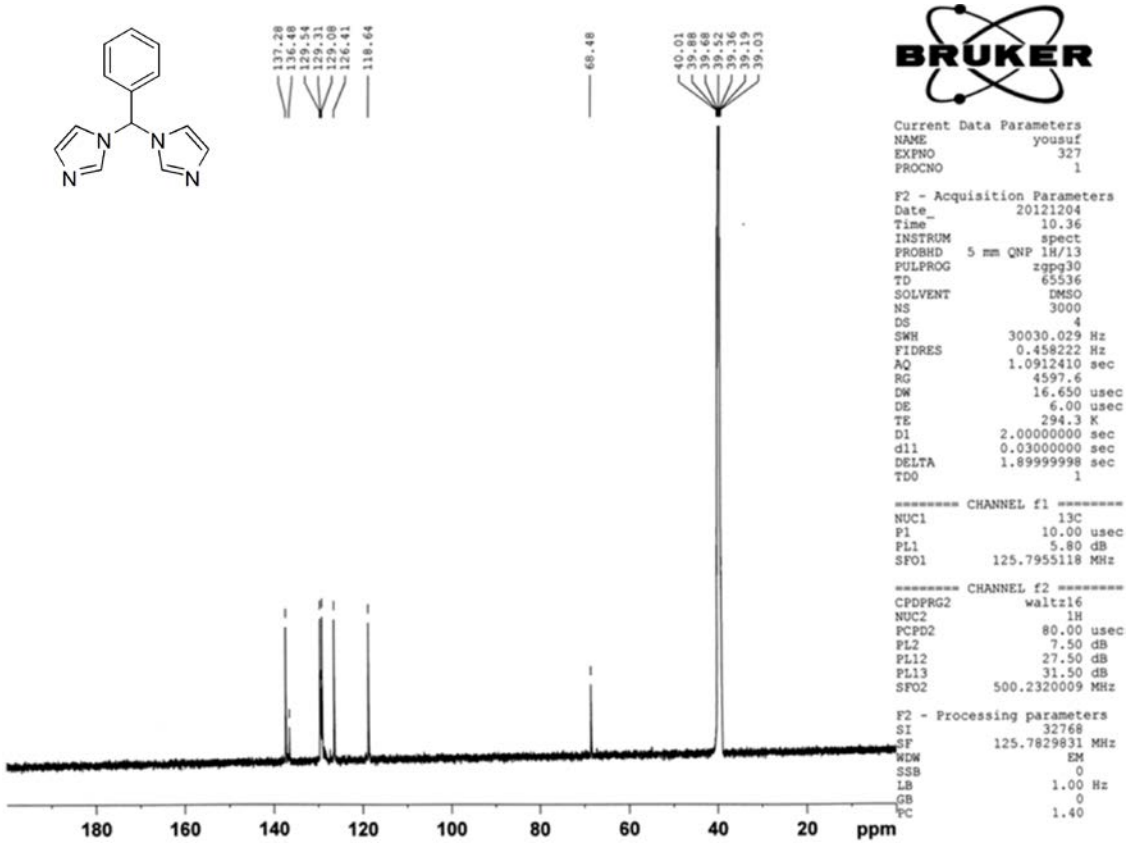

Figure S2. [13]C NMR spectrum of compound 1,1'-(phenylmethylene)bis(1H-imidazole) DMSO-d_6.

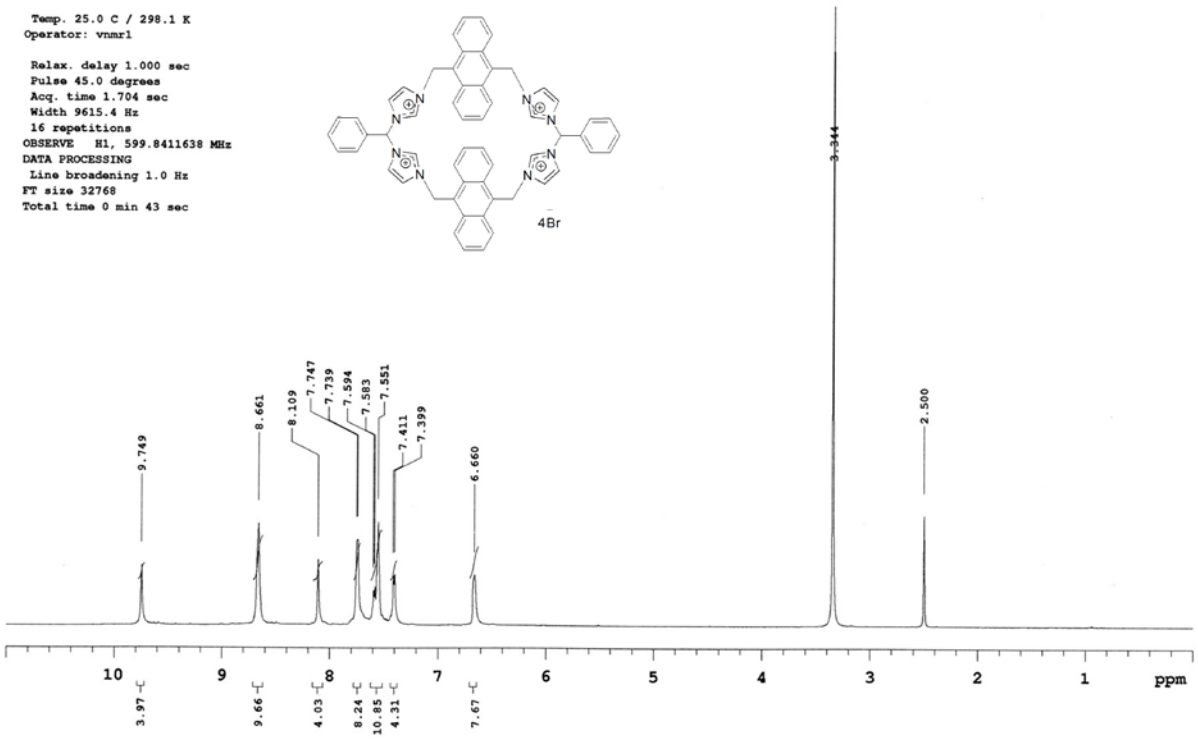

Figure S3. ^{1}H NMR spectrum of compound (**1**) in DMSO-d_6.

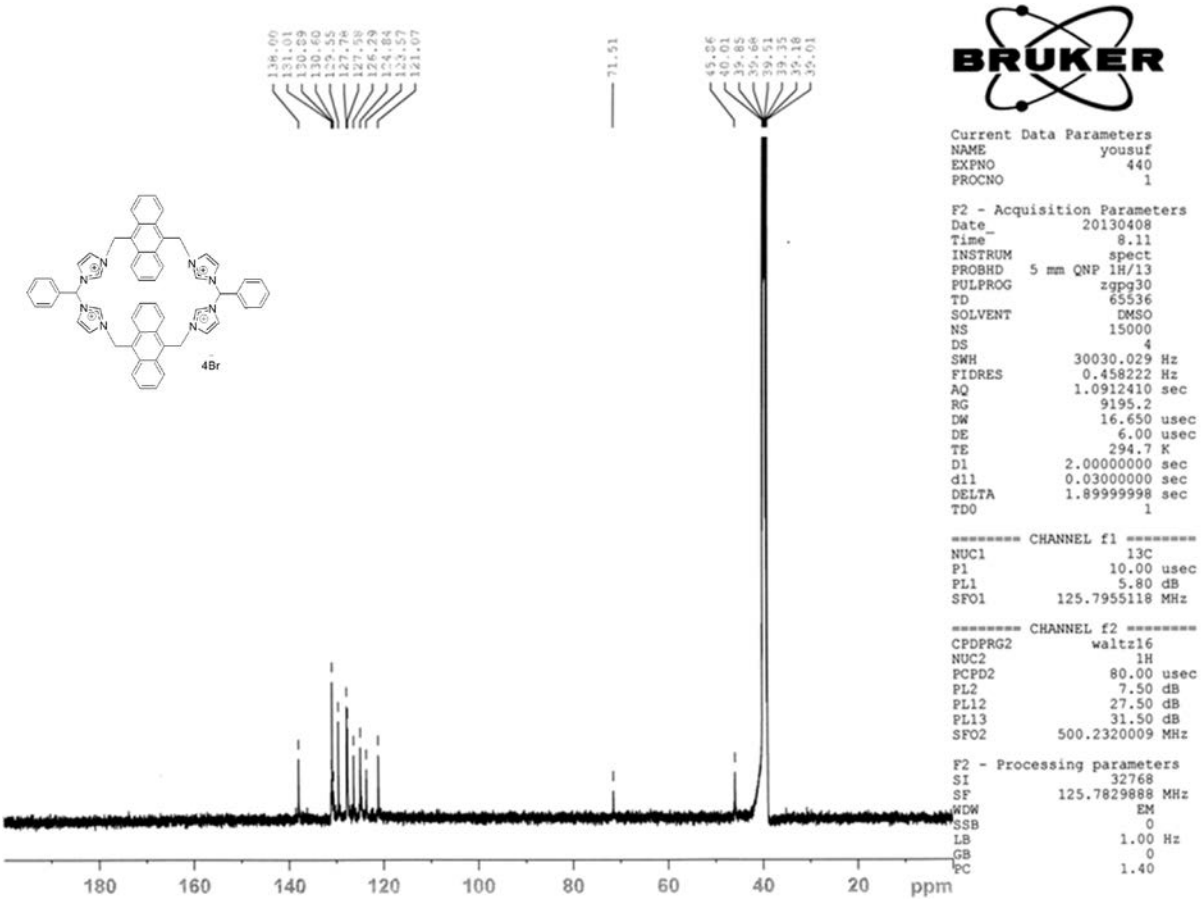

Figure S4. ^{13}C NMR spectrum of compound (**1**) in DMSO-d_6.

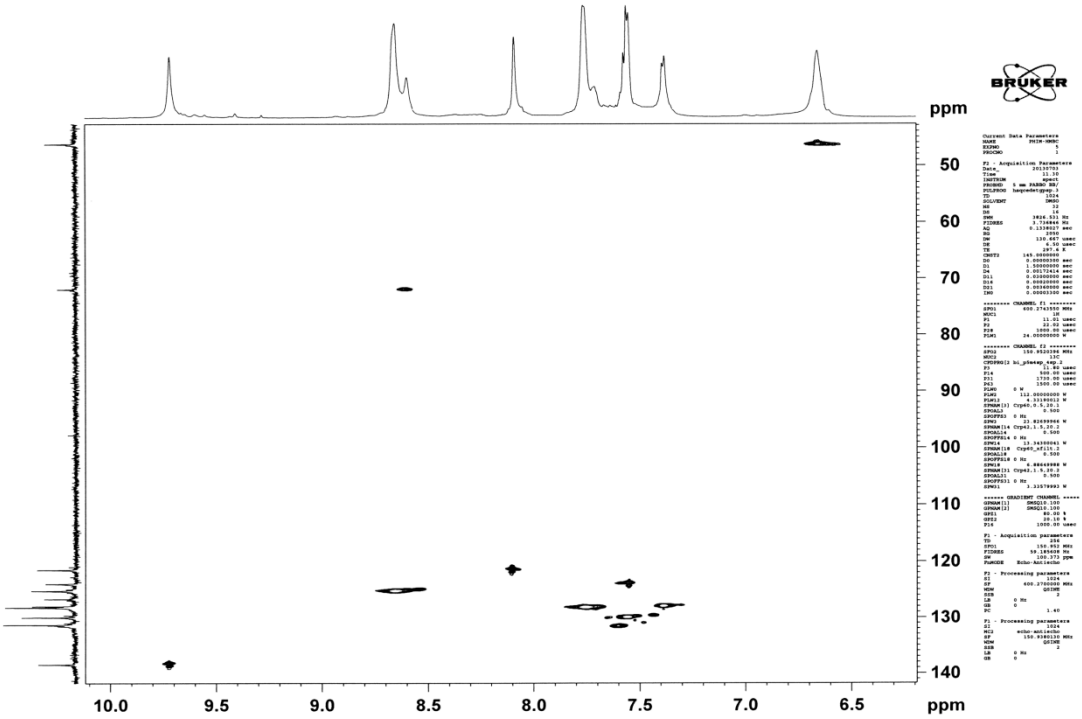

Figure S5. 600 MHz HSQC spectrum of **1** with in DMSO-d_6.

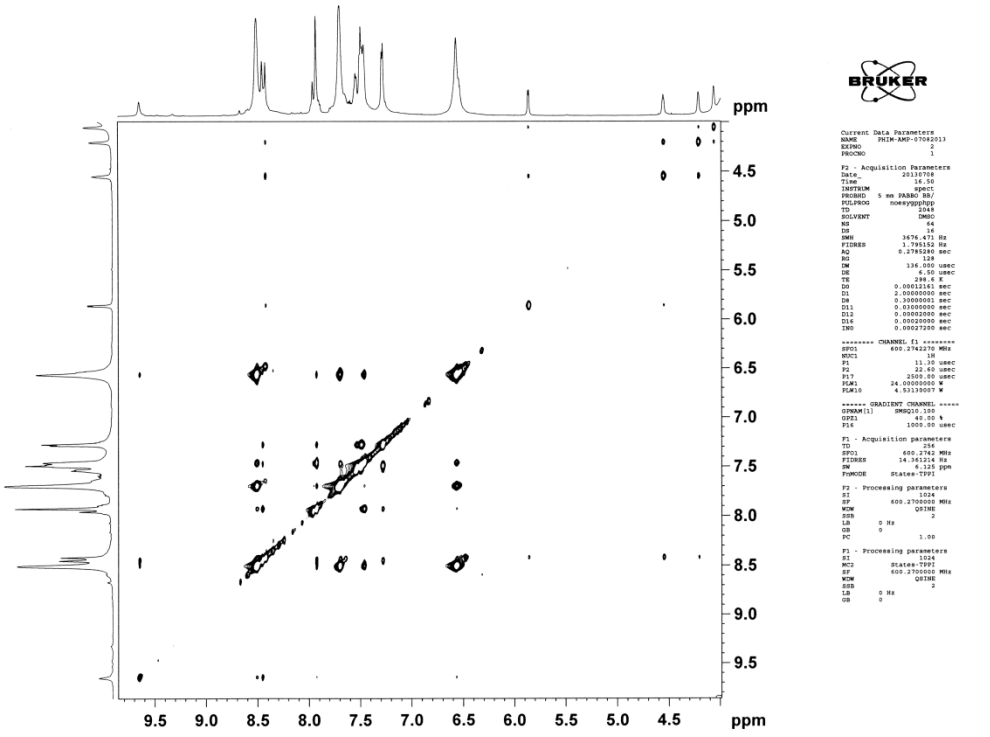

Figure S6. 600 MHz NOESY spectrum of **1** with 1 eq. of AMP in DMSO-d_6.

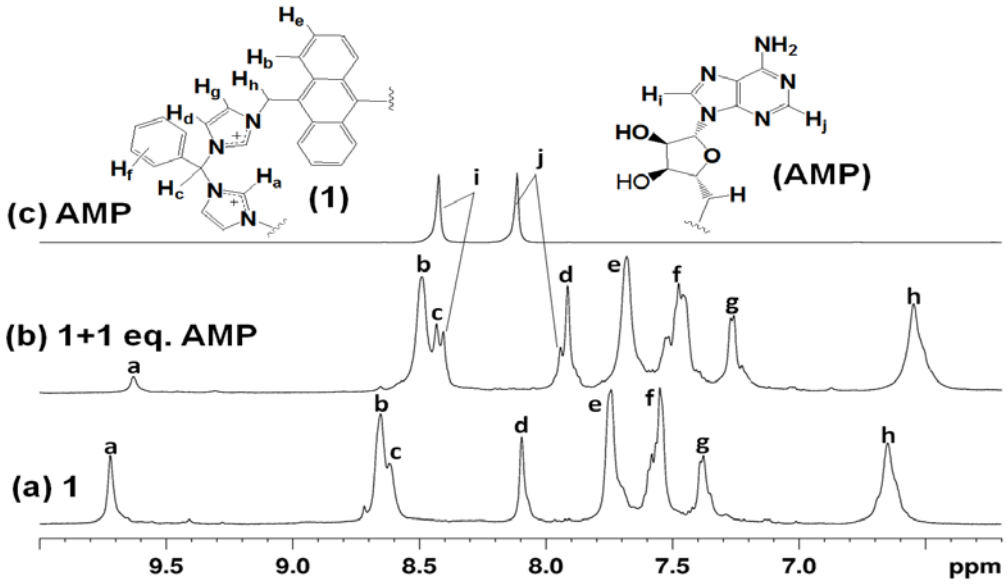

Figure S7. Partial 500 MHz ^{1}H NMR spectra for (a) **1** (2 mM), (b) **1**-AMP (1 equiv), and (c) AMP. AMP was dissolved in D_2O as stock solution.

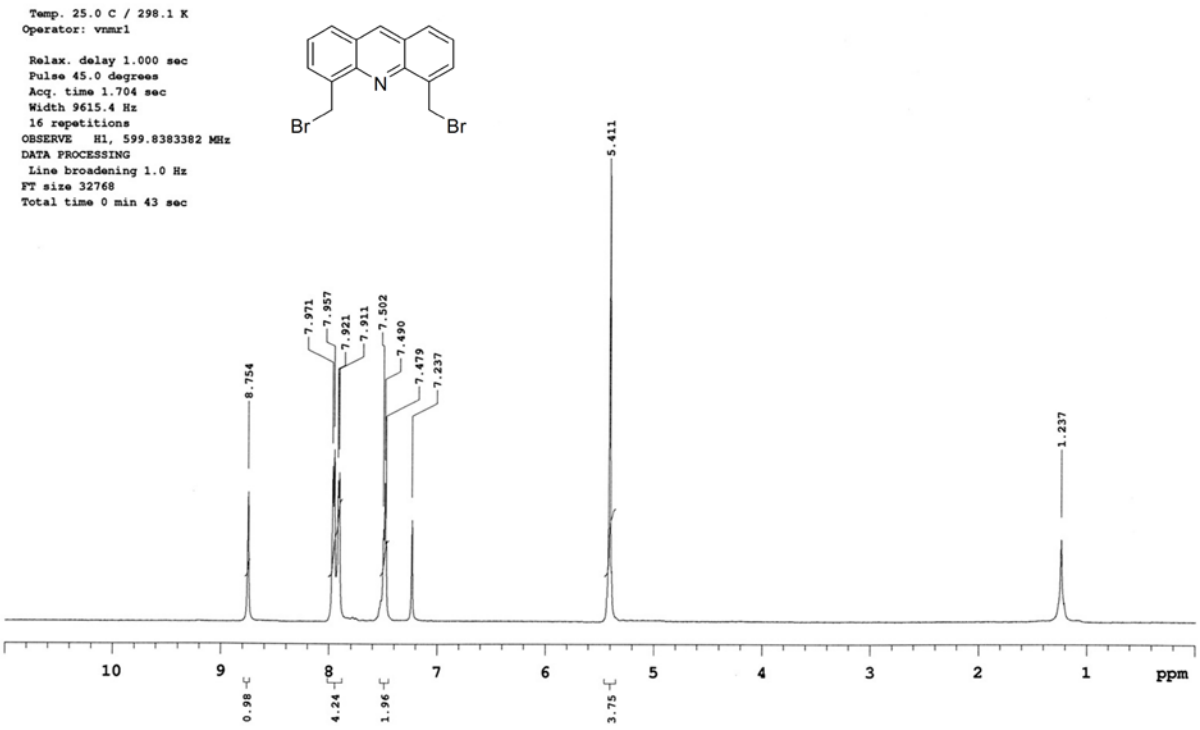

Figure S8. ^{1}H NMR spectrum of compound 4,5-bis(bromomethyl) acridine in $CDCl_3$.

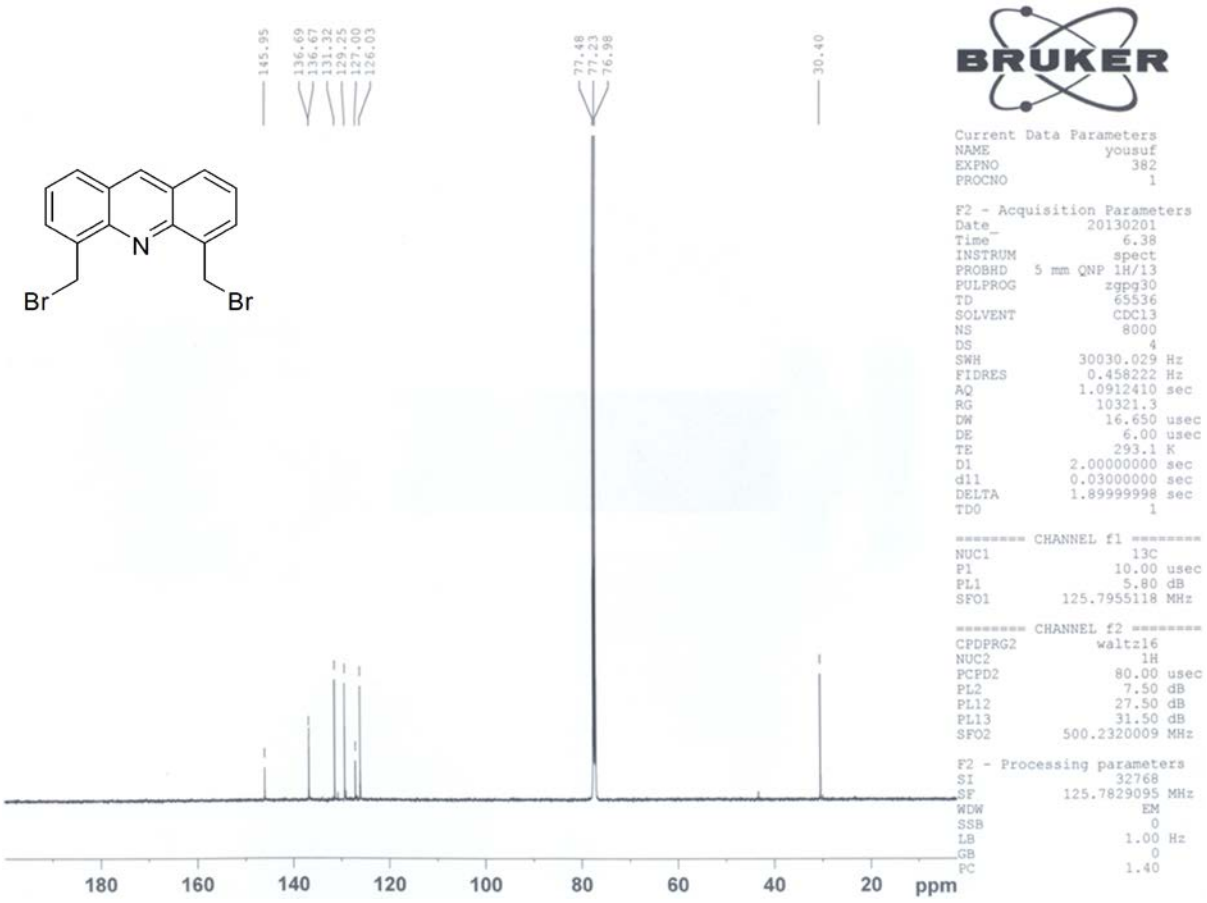

Figure S9. ^{13}C NMR spectrum of compound 4,5-bis(bromomethyl) acridine $CDCl_3$.

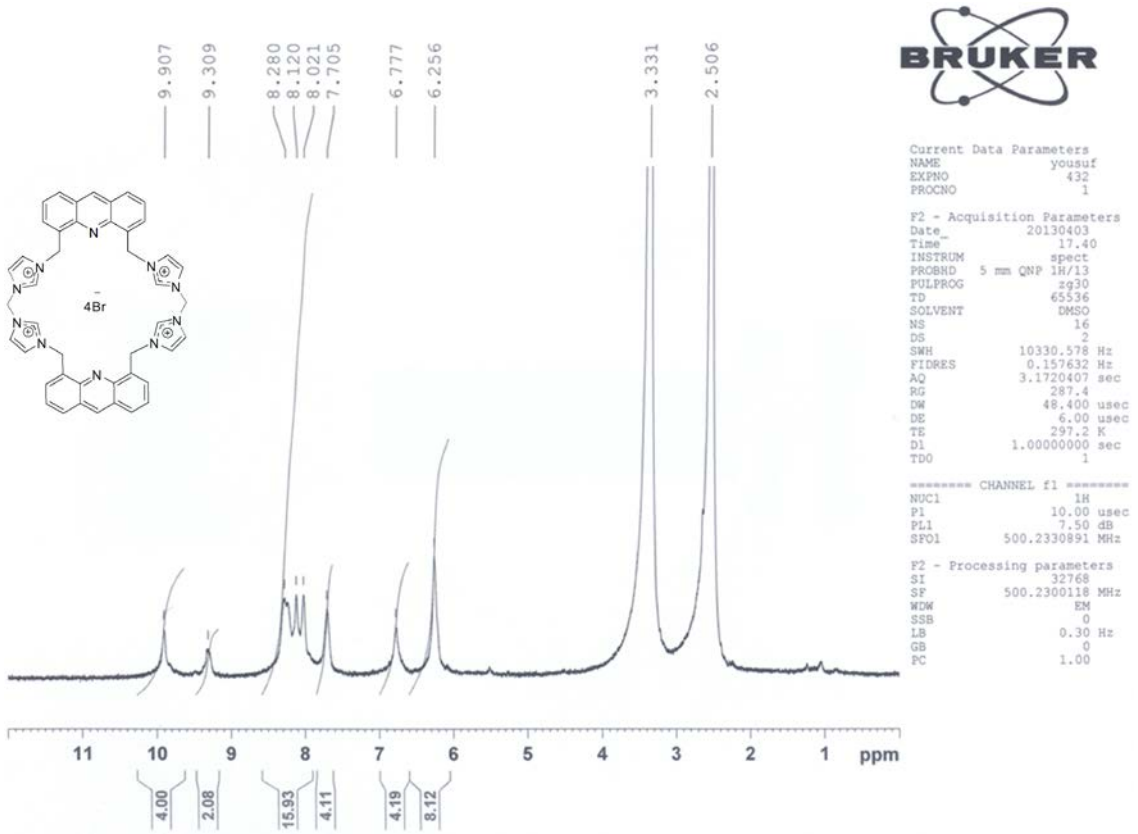

Figure S10. [1]H NMR spectrum of compound **2** in DMSO-d_6.

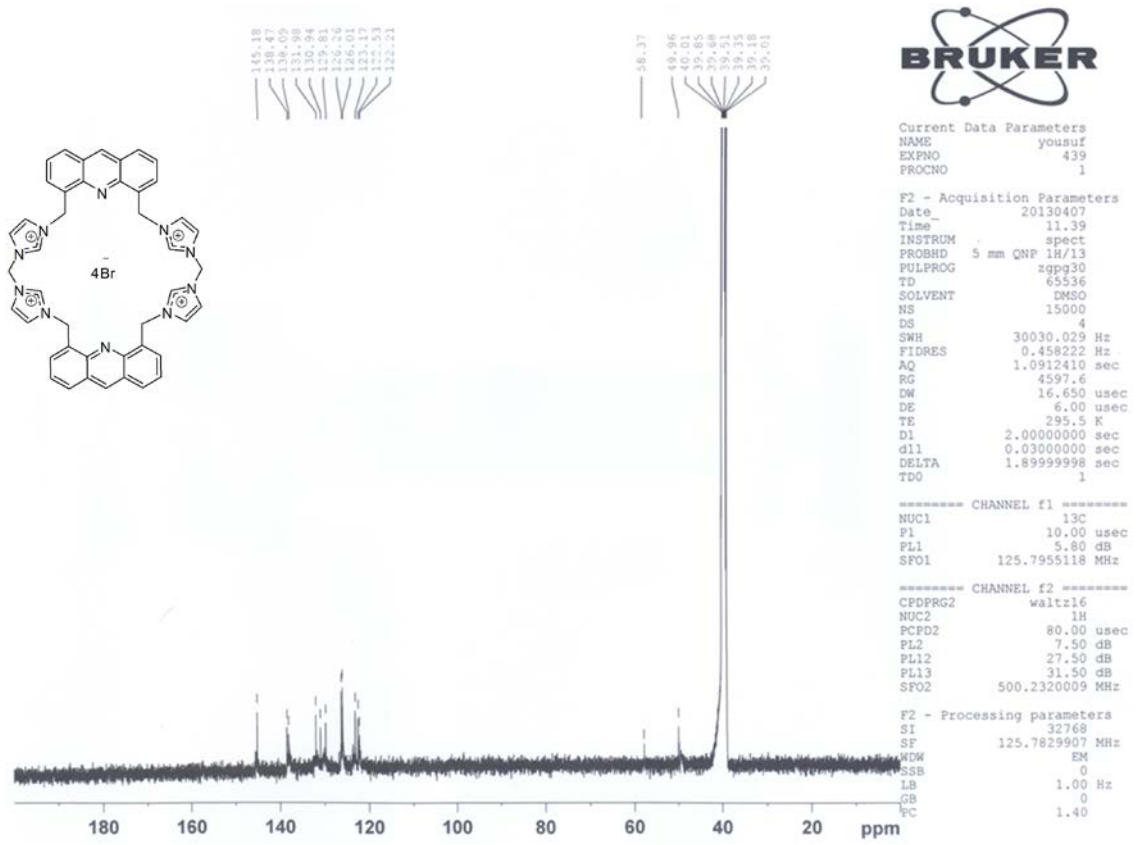

Figure S11. [13]C NMR spectrum of compound **2** in DMSO-d_6.

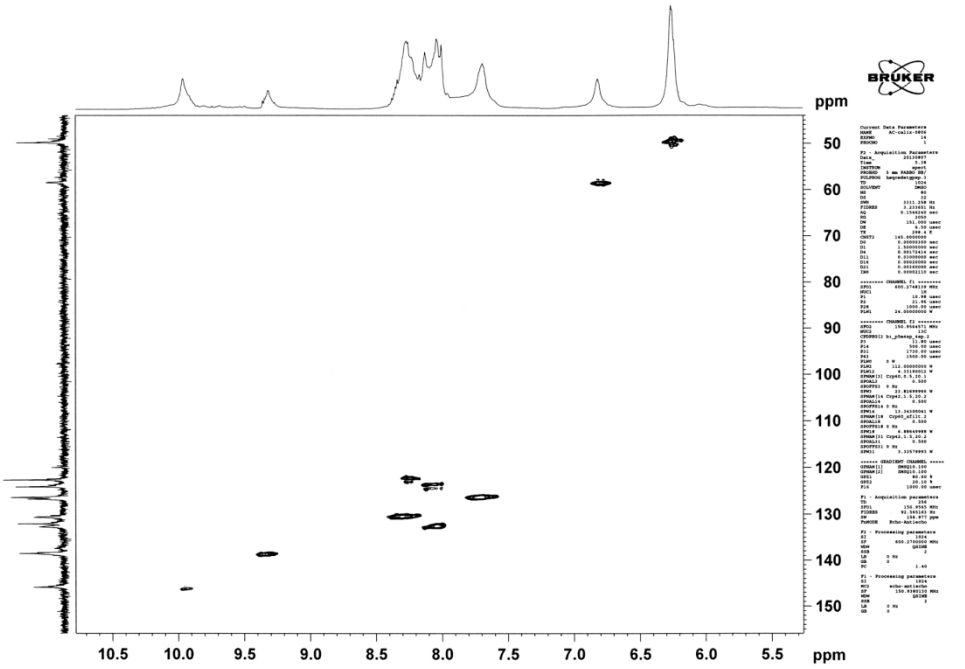

Figure S12.HSQC spectrum of compound **2** in DMSO-d_6.

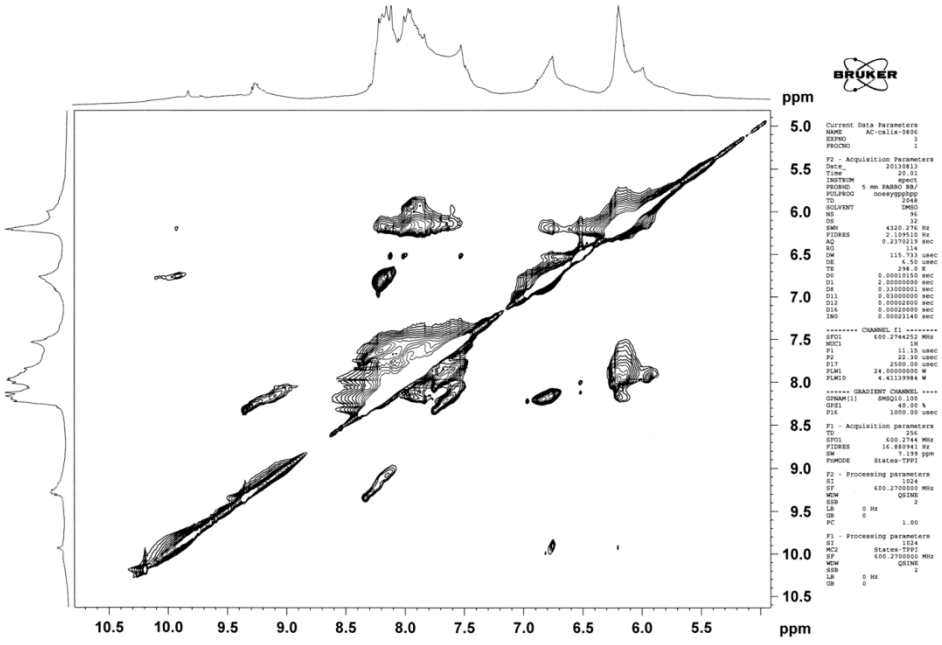

Figure S13. 600 MHz NOESY spectrum of **2** with 1 eq. of GTP in DMSO-d_6.

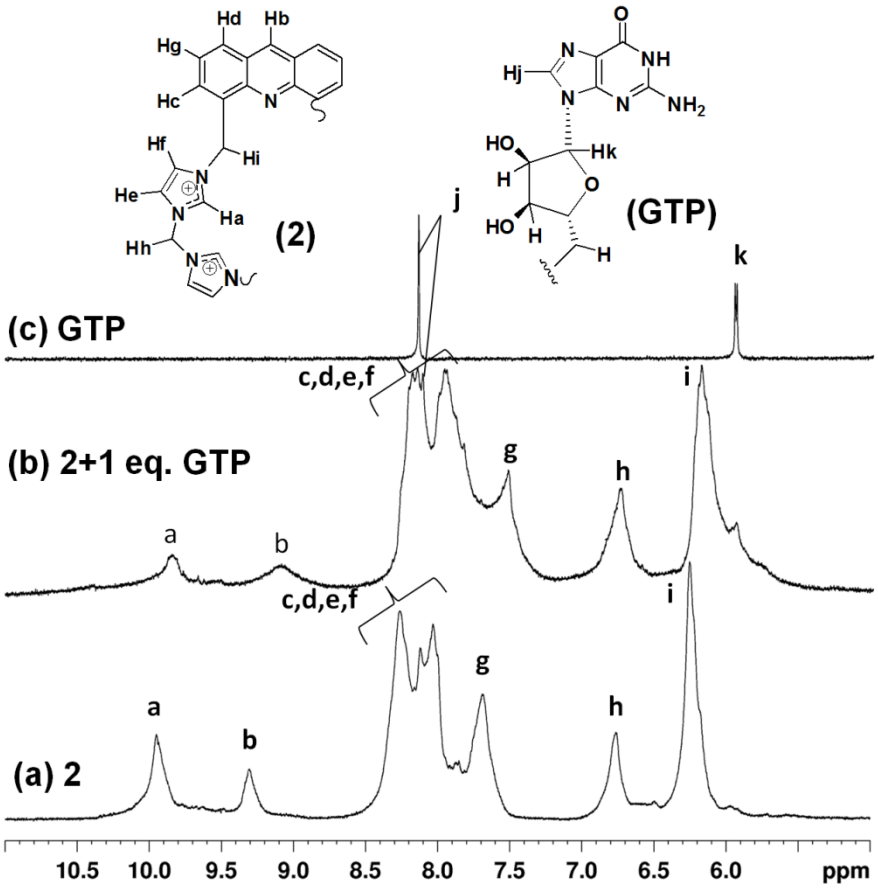

Figure S14. Partial 500 MHz ^{1}H NMR spectra for (a) **2** (2 mM), (b) **2**-GTP (1 equiv), (c) GTP. GTP was dissolved in D_2O as stock solution.

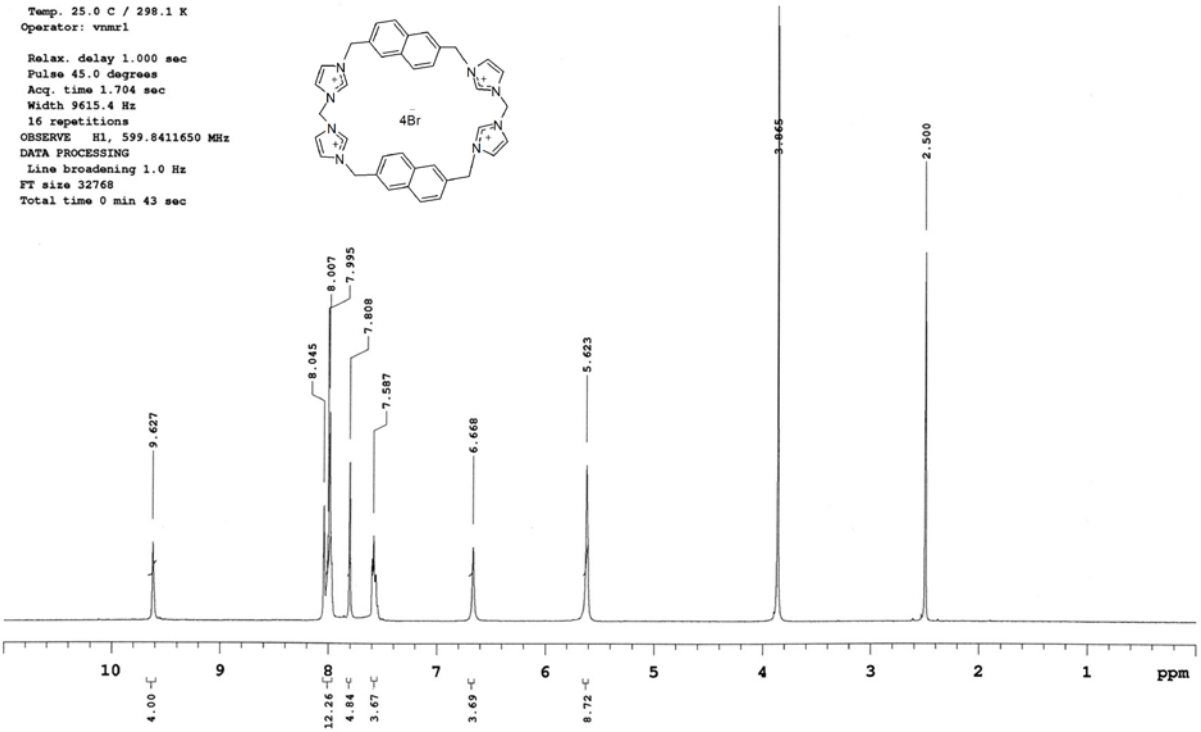

Figure S15. ^{1}H NMR spectrum of compound **3** in DMSO-d_6

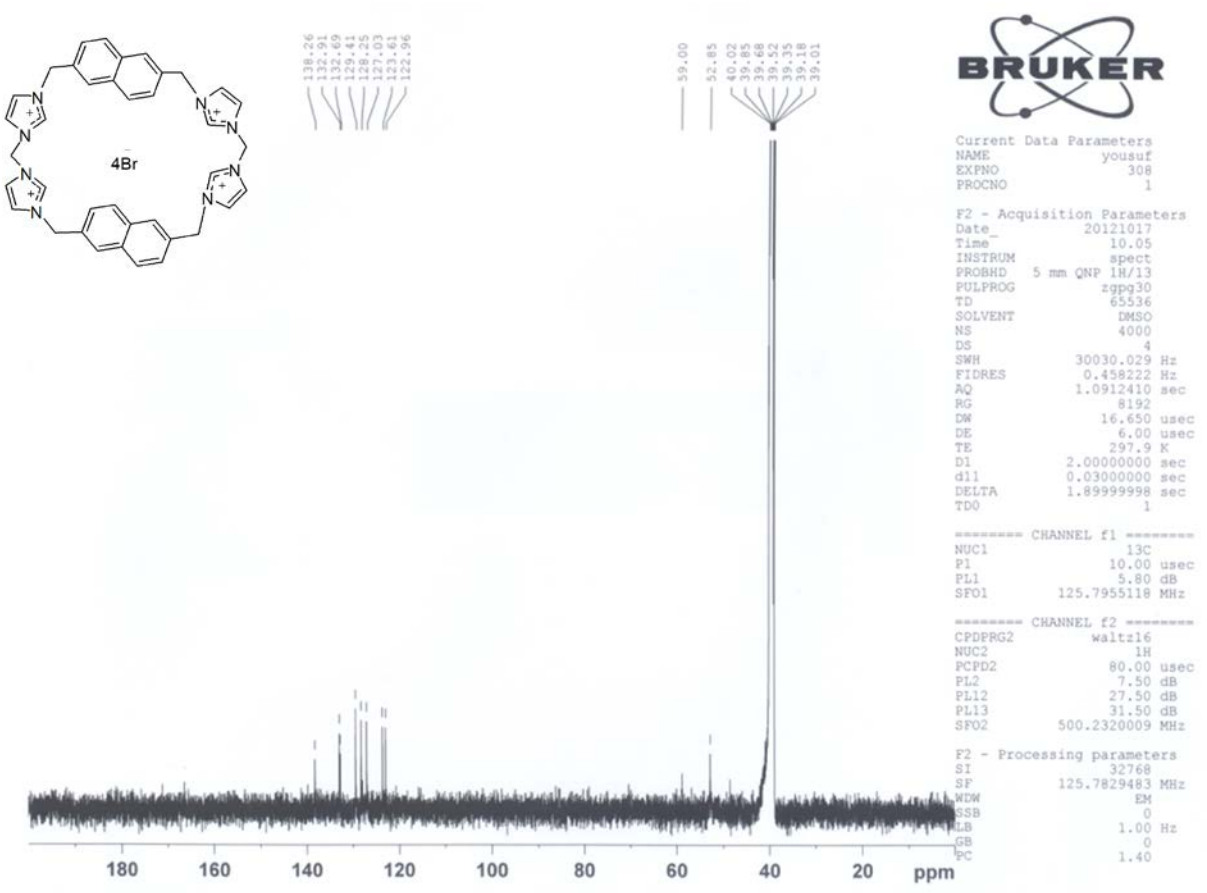

Figure S16. ^{13}C NMR spectrum of compound **3** in DMSO-d_6

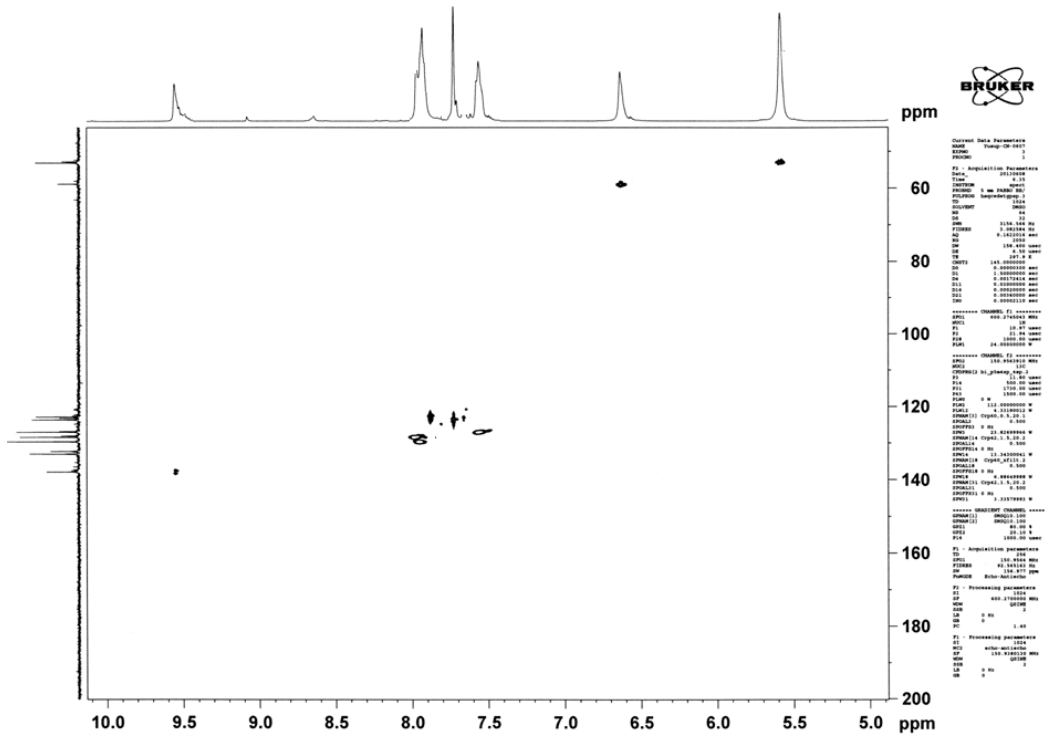

Figure S17. HSQC spectrum of compound **3** in DMSO-d_6

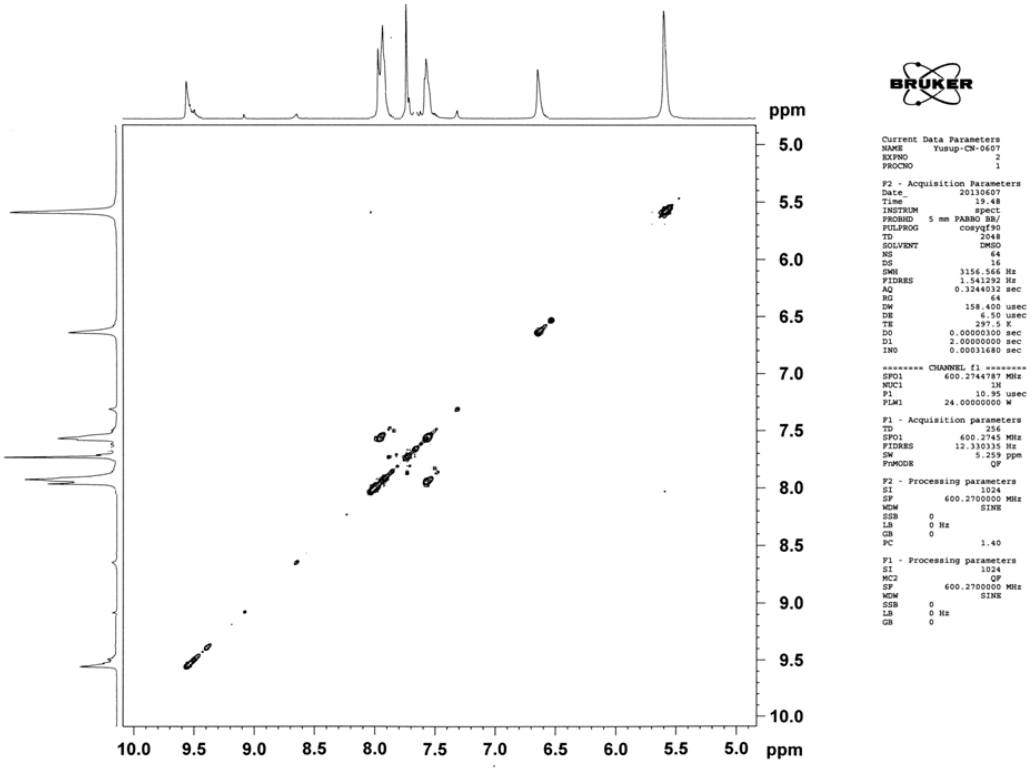

Figure S18. ^{1}H COSY spectrum of compound **3** in DMSO-d_6

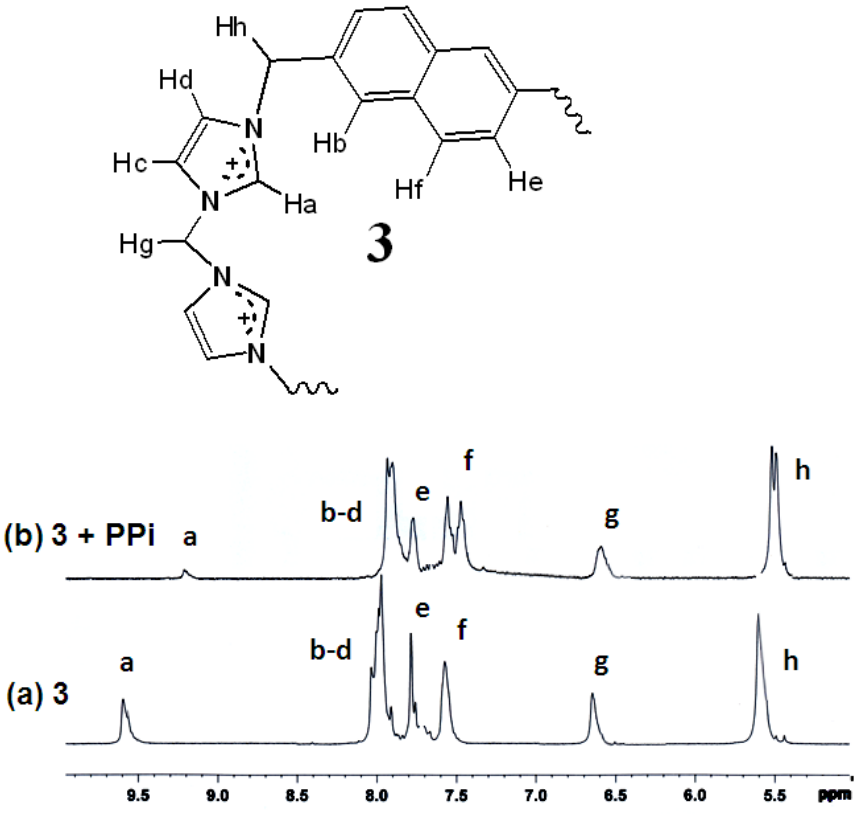

Figure S19. Partial 500 MHz ^{1}H NMR spectra for (a) **3** (2 mM), (b) **3**-PPi (1 equiv).PPi was dissolved in D_2O as stock solution.

1. Fluorometric Analysis:

All spectrofluorimetric titrations were performed as follows. Stock solution of compound (**1**, **2** or **3**) (1mM) was prepared at pH 7.4 in 0.01 M HEPES buffer water mixture and used in the preparation of titration solution by appropriate dilution up to 10 μM. Aliquots of F^-, Cl^-, I^-, $CH_3CO_2^-$, NO_3^-, Pi, PPi, AMP, ADP, ATP, GMP, GDP, GTP, CMP, CTP, UMP, UTP, TMP and TTP (as the corresponding tetrabutyl ammonium and sodium salts) in 0.01 M HEPES buffer water mixture was then injected into the sample solution through a rubber septum in the cap. To account for dilution effects, these stock anion solutions also contained the receptors at its initial concentration. The sample solutions were magnetically stirred for 1 minute after each addition before rescaning. This process was repeated until the change in fluorescence intensity became insignificant. Binding constants K_a for anions were derived from the plots of F/F_0 vs [anion] by assuming one site model using Origin Lab 8.0.[1] Results reported in the main text are the average of at least two independent titrations. Emission spectrum was measured by keeping slit width = 5 nm and λ_{exc}= 365 nm.

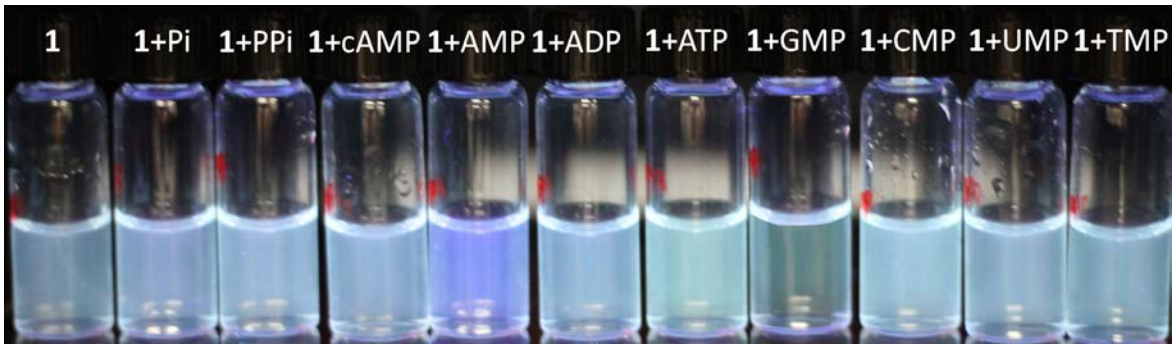

Figure S20. Visual fluorescence features of **1** (10 µM) upon the addition of *n*-tetrabutylammomonium (TBA) salts; dihydrogen phosphate (Pi), pyrophosphate (PPi) and sodium salt of AMP, cAMP, ADP, ATP, GMP, GTP, CMP, CTP, UMP, UTP, TMP and TTP (100 equiv) at pH 7.4 (0.01 M HEPES buffer).

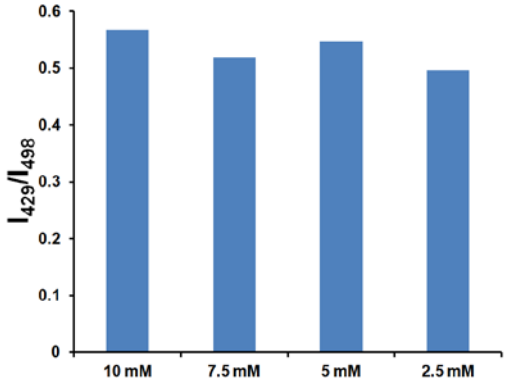

Figure S21. The emission intensity ratio of cyclophane **1** at I_{429}/I_{498} in 0.01M HEPES buffer at 10, 7.5, 5 and 2.5 mM (slit width = 5 nm; excitation at 365 nm). The concentration independent changes in monomer-to-excimer (I_{429}/I_{498}) ratio indicate intamolecular excimer formation.

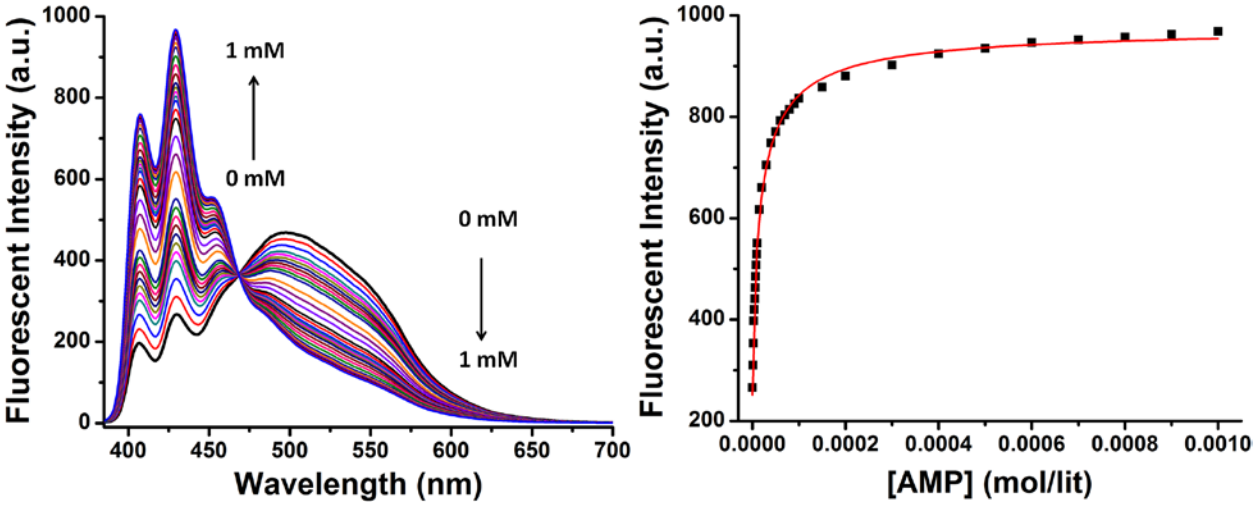

Figure S22. Emission spectra (excitation at 365 nm) of receptor **1**(10 μM) upon addition of sodium salt of AMP at pH 7.4 (0.01 M HEPES buffer, 25^{o}C) and the corresponding binding isotherm.

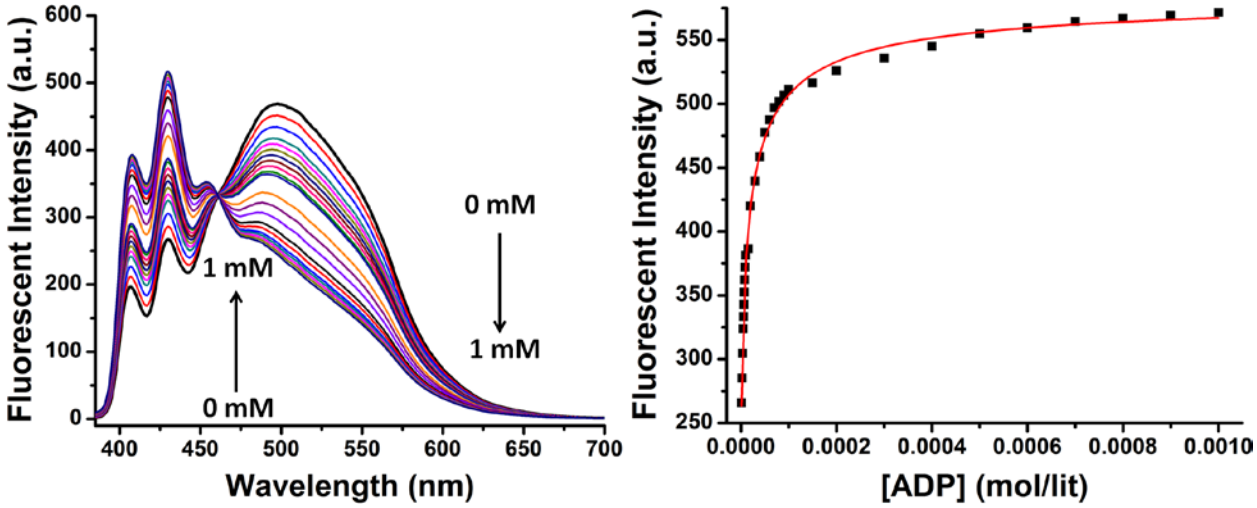

Figure S23. Emission spectra (excitation at 365 nm) of receptor **1**(10 μM) upon addition of sodium salt of ADP at pH 7.4 (0.01 M HEPES buffer, 25^{o}C) and the corresponding binding isotherm.

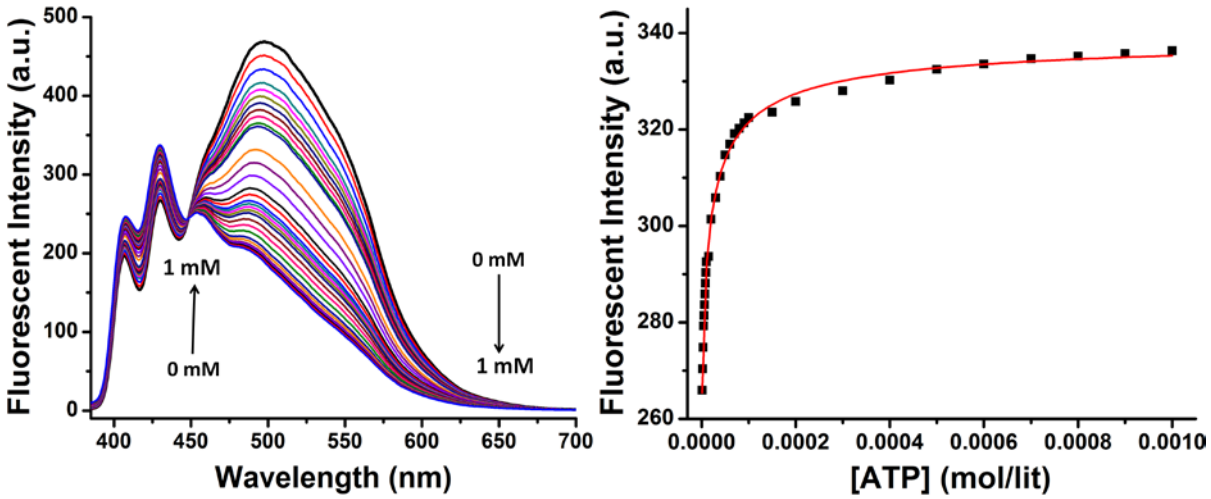

Figure S24. Emission spectra (excitation at 365 nm) of receptor **1** (10 μM) upon addition of sodium salt of ATP at pH 7.4 (0.01 M HEPES buffer, 25°C) and the corresponding binding isotherm.

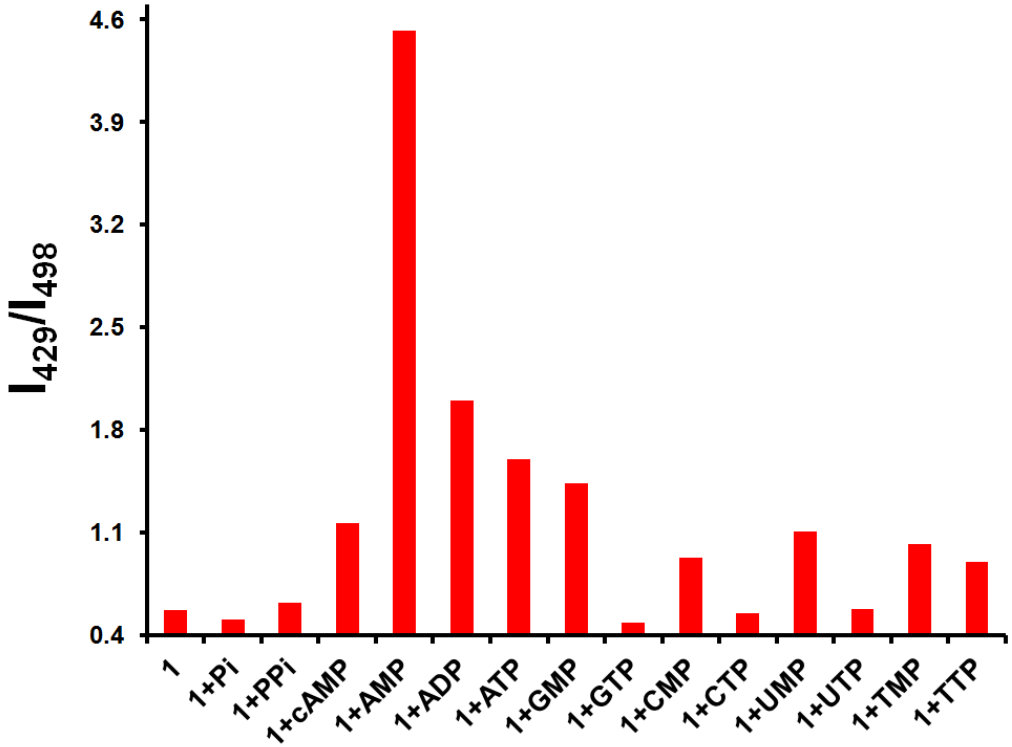

Figure S25. Plot of monomer to excimer ratio (I_{429}/I_{498}) of **1** and with addition (100 equiv) of different anions.

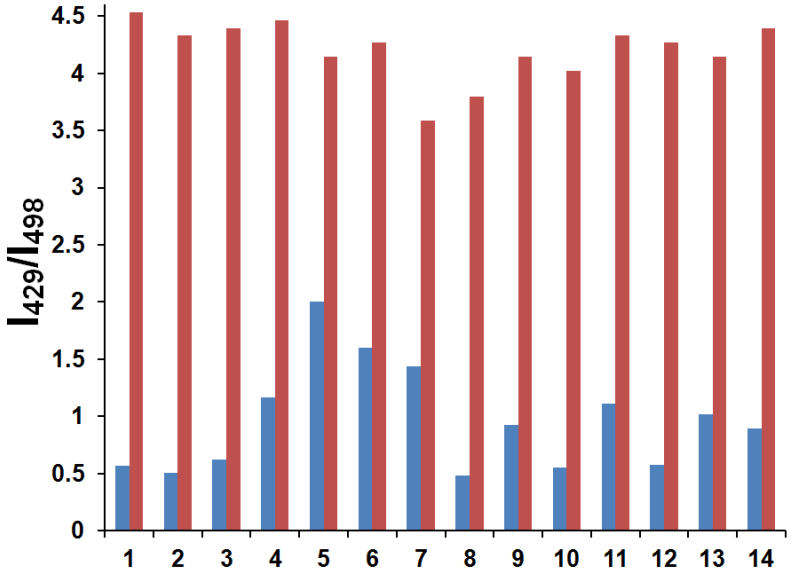

Figure S26. Fluorescence response of **1** to various anions at pH 7.4 (0.01M HEPES) (excitation at 365 nm). Blue bars represent the addition of 10 equivalent of the appropriate anion to 10 μM solution of **1**. Red bars represent the subsequent addition of 10 equivalent of AMP to the solution. (1) No anion, (2) Pi, (3) PPi, (4) cAMP, (5) ADP, (6) ATP, (7) GMP, (8) GTP, (9) CMP, (10) CTP, (11) UMP, (12) UTP, (13) TMP, (14) TTP.

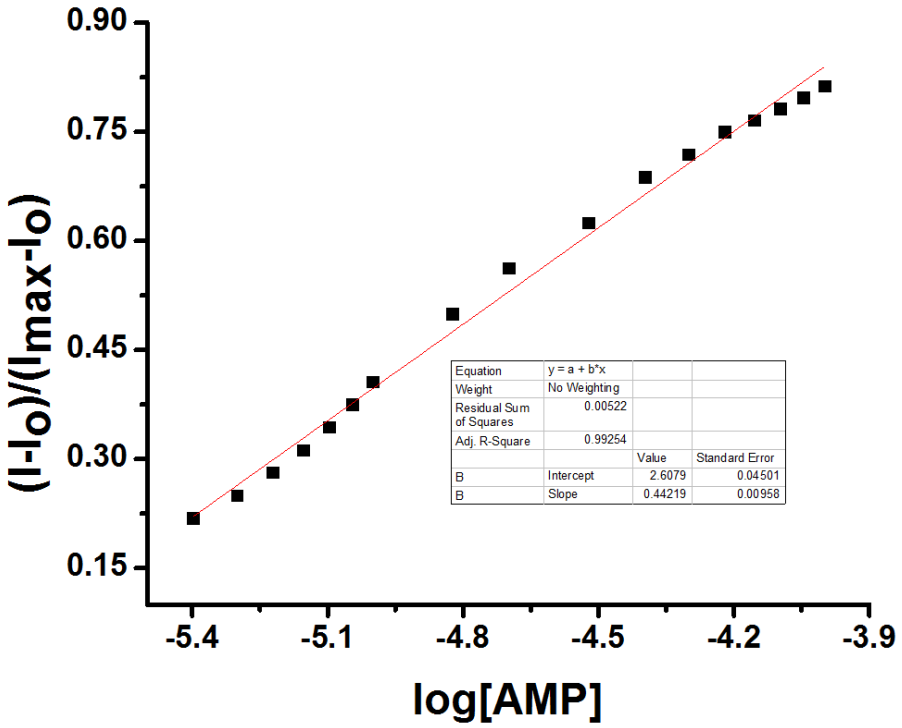

Figure S27 A plot of (Fo-F)/(Fo-Fmax) vs log[AMP].

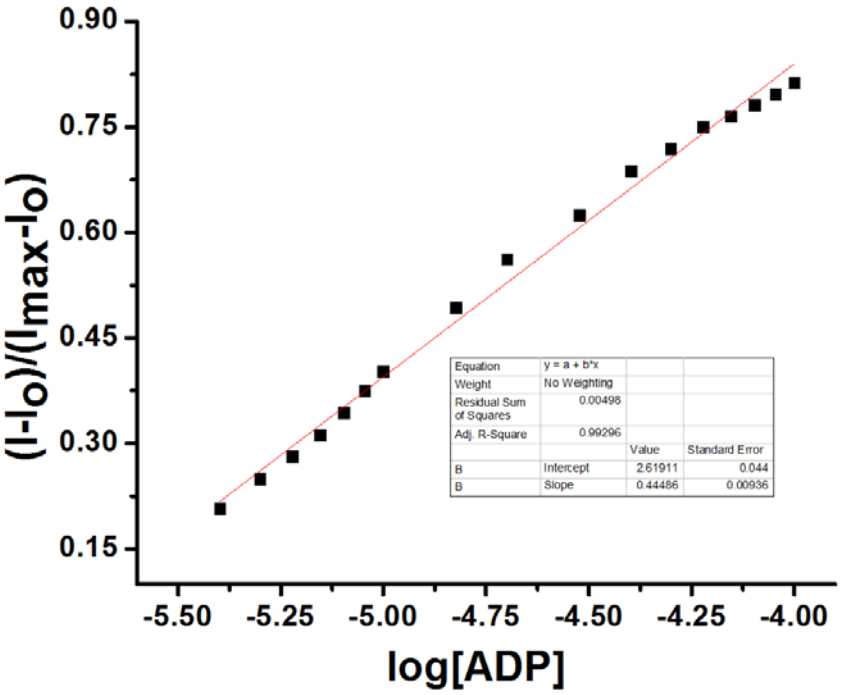

Figure S28. A plot of (Fo-F)/(Fo-Fmax) vs log[ADP].

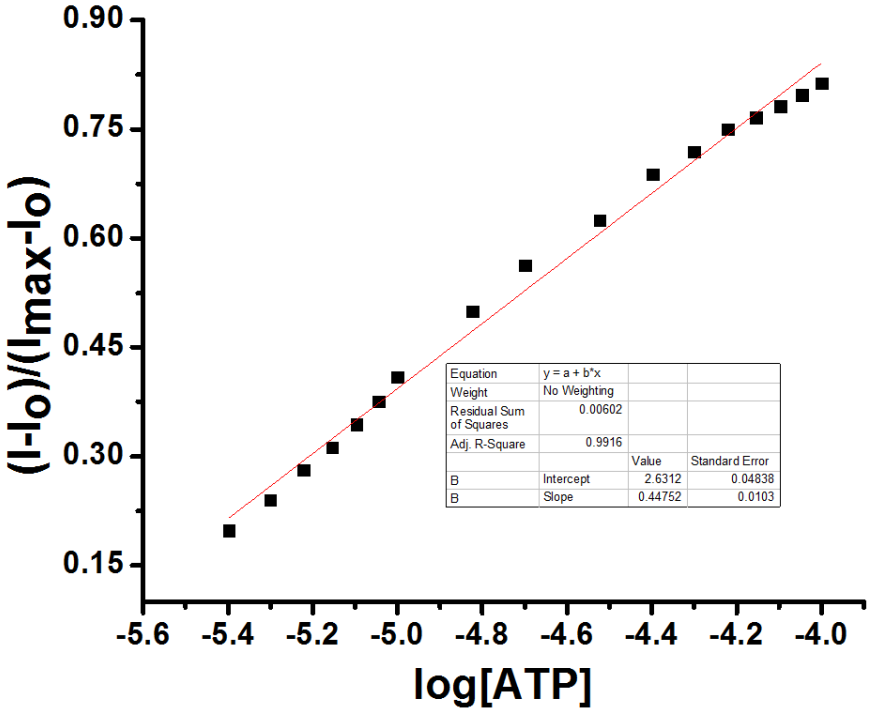

Figure S29. A plot of (Fo-F)/(Fo-Fmax) vs log[ATP].

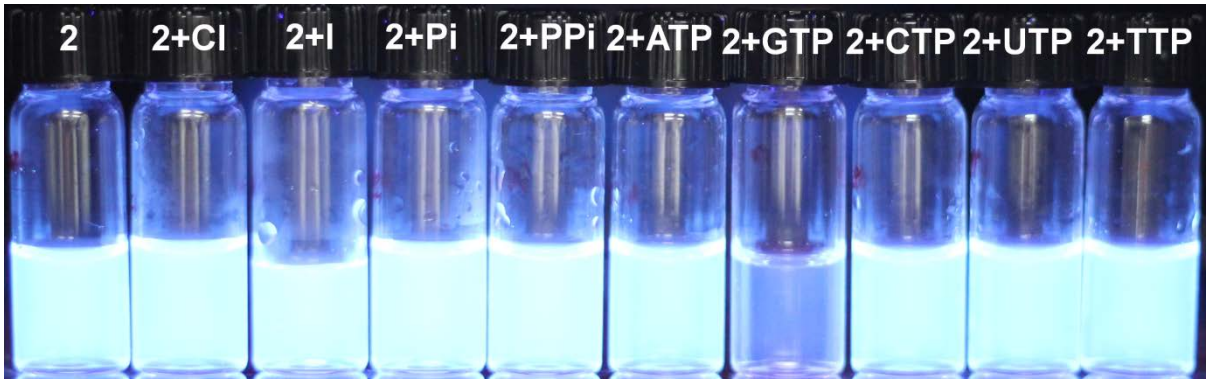

Figure S30. Visual fluorescence features of **2** (10 μM) upon the addition of *n*-tetrabutylammomonium (TBA) salts; of Cl^-, I^-, dihydrogen phosphate (Pi), pyrophosphate (PPi) and sodium salt of ATP, GTP, CTP, UTP and TTP (10 equiv) at pH 7.4 (10 mM HEPES buffer).

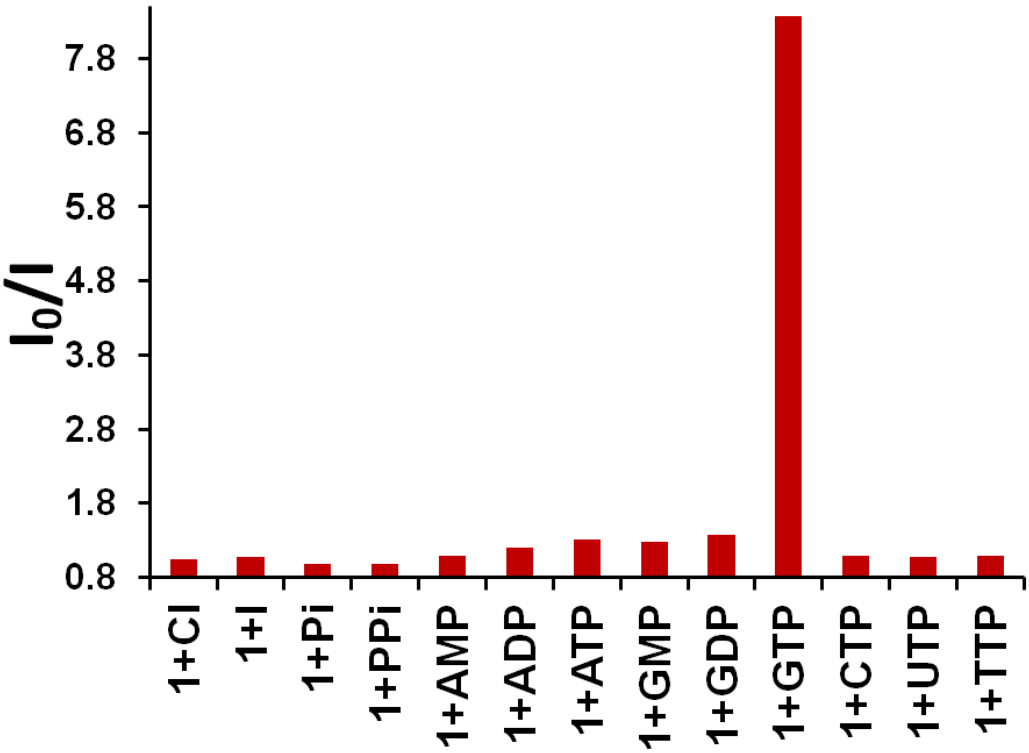

Figure S31. Effect of different anions (10 equiv) on I_o/I of probe **2** at a fixed concentration of 10μM at pH 7.4 (10mM HEPES buffer) (slit width = 5 nm; λ_{exc}=365 nm).

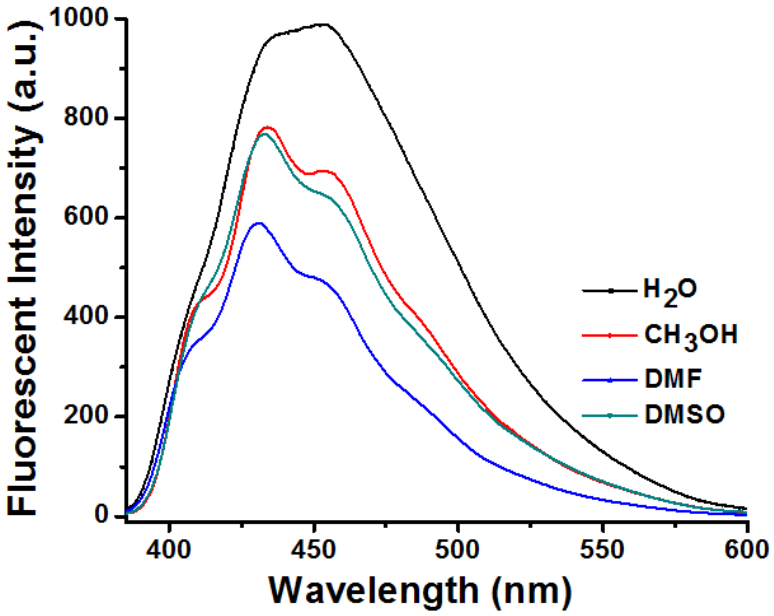

Figure S32. Emission spectra (excitation at 365 nm) of probe **2** (10 μM) in different solvents.

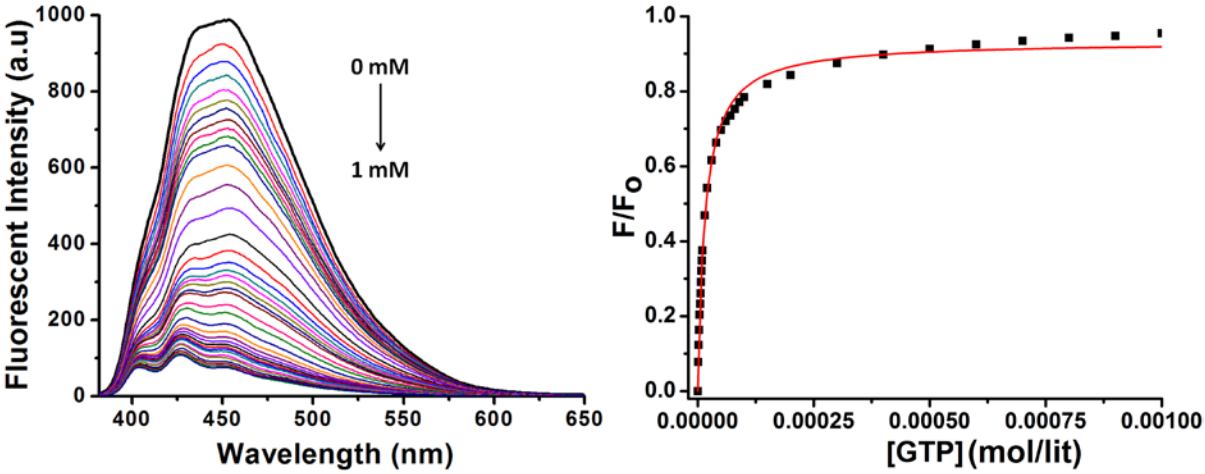

Figure S33. Emission spectra (excitation at 365 nm) of probe **2** (10 μM) upon addition of sodium salt of GTP at pH 7.4 (10 mM HEPES buffer, 25ºC) and the corresponding binding isotherm.

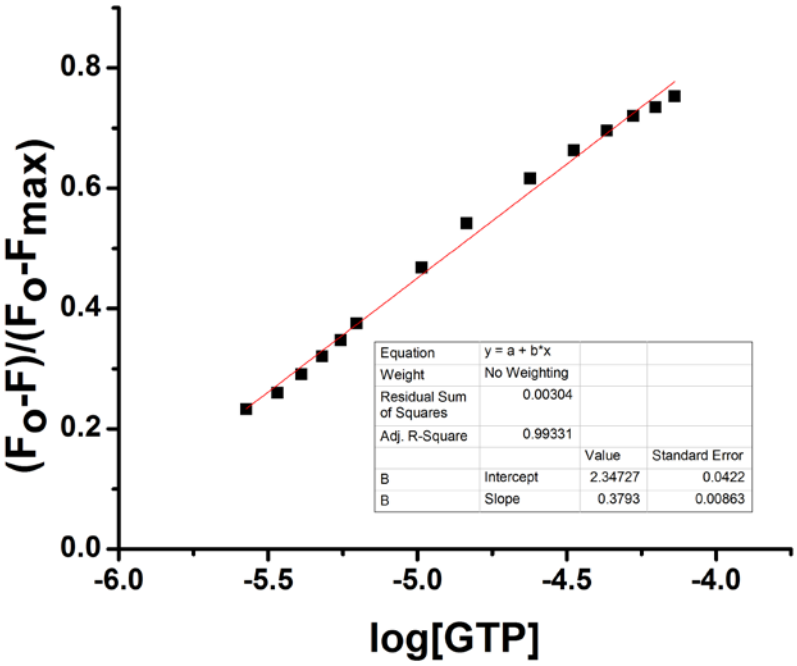

Figure S34. A plot of (Fo-F)/(Fo-Fmax) vs log[GTP].

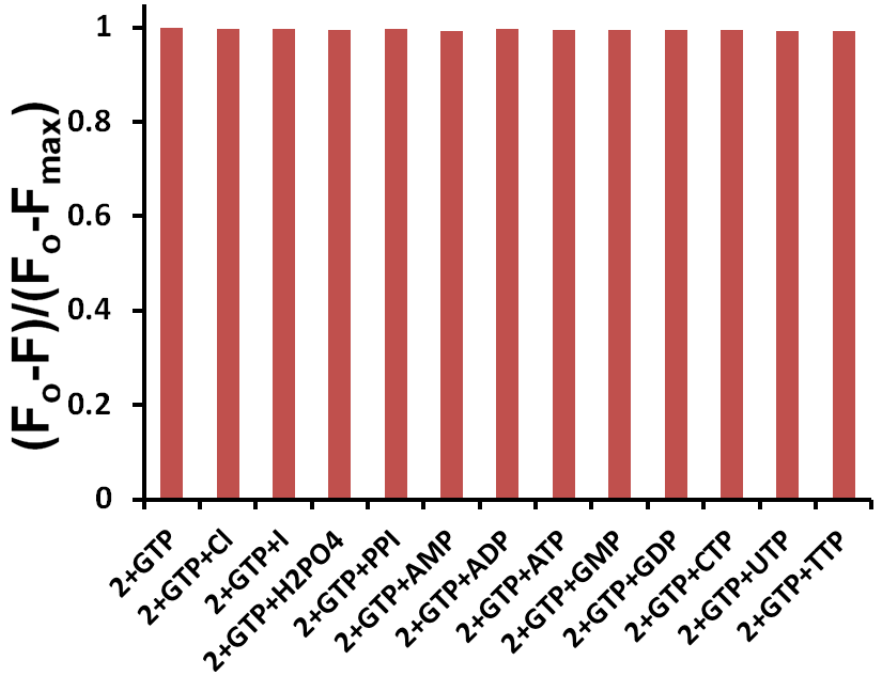

Figure S35. Competitive experment in the **2**+GTP system with interfering anions. [**2**] = 10 μM, [GTP] = 100 μM, and [A^-] = 100 μM in 10mM HEPES buffer; λ_{ex} = 365 nm.

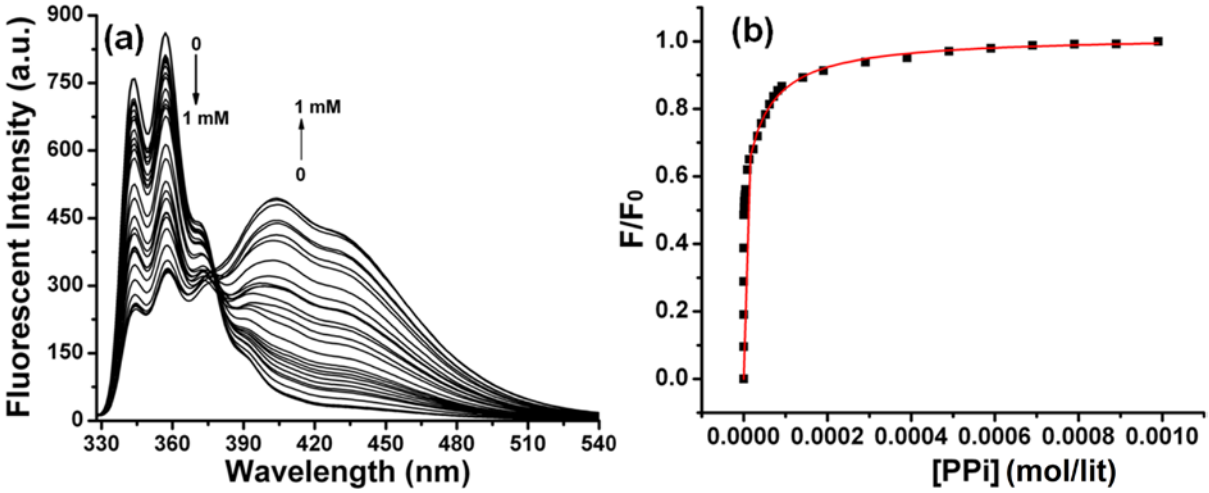

Figure S36. Emission spectra (excitation at 290 nm) of receptor **3** (10 µM) upon addition of *n*-TBA salt of PPi at pH 7.4 (10 mM HEPES buffer) and the corresponding binding isotherm.

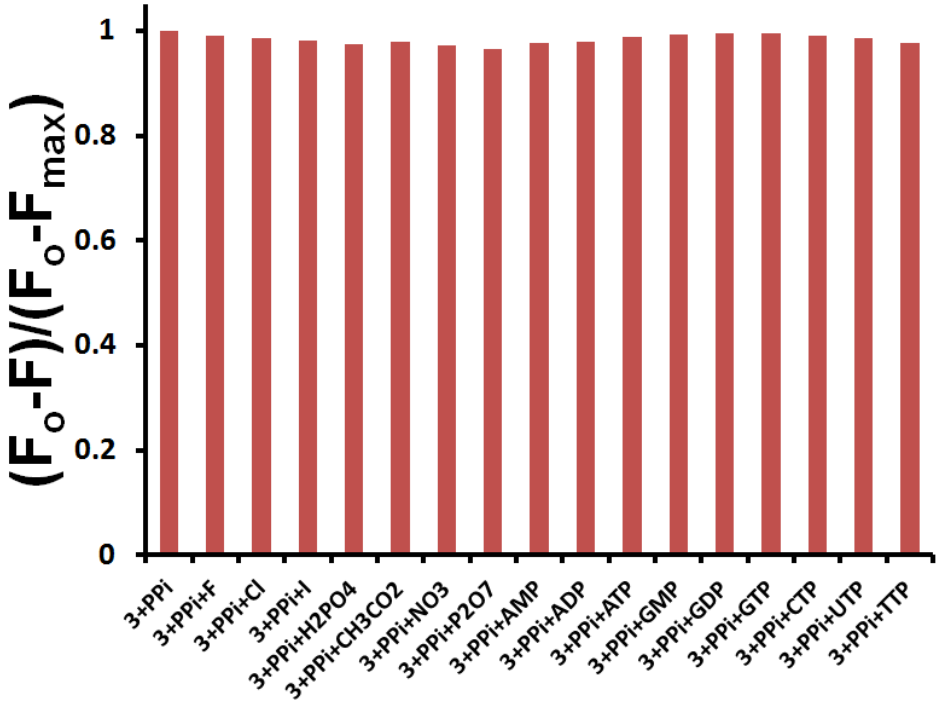

Fig.37. Competitive experiment in the **3** + PPi with interfering anions. [**3**]= 10 µM , [PPi] = 0.1 mM, and [A^-]= 0.1 mM in 10 mM HEPES buffer. (slit width = 5 nm; λ_{ex} = 290).

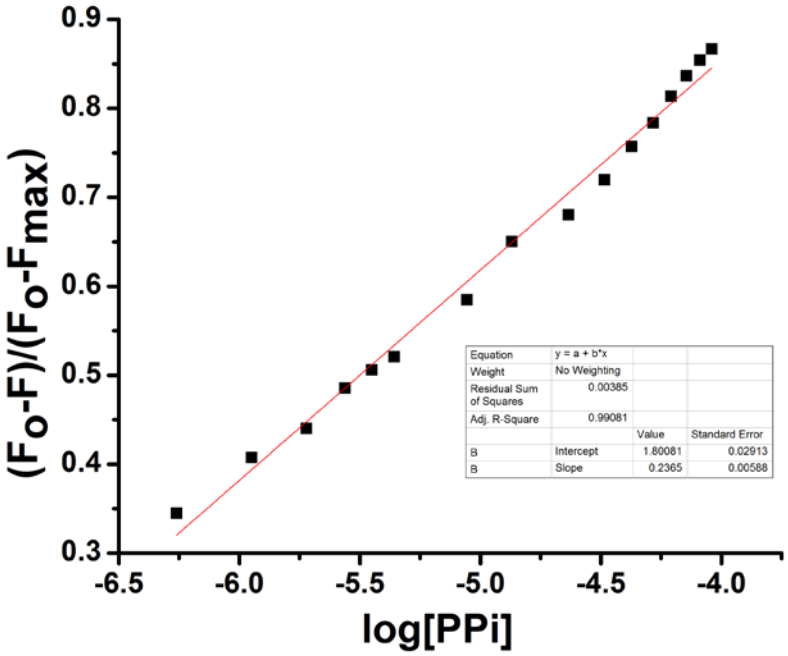

Figure S38. A plot of (Fo-F)/(Fo-Fmax) vs log[PPi].

Studies of receptor-anion complex stoichiometry (Job plot)

Job plot analysis was performed using fluorescence emission spectroscopy. The plot was constructed in the usual way and was found to exhibit maxima at 0.5 for AMP, 0.5 for GTP and 0.66 for PPi. Such finding supports the proposal that receptors **1** and **2** form a 1:1 complex with the AMP and GTP respectively while receptors **3** forms 2:1 complex with PPi.

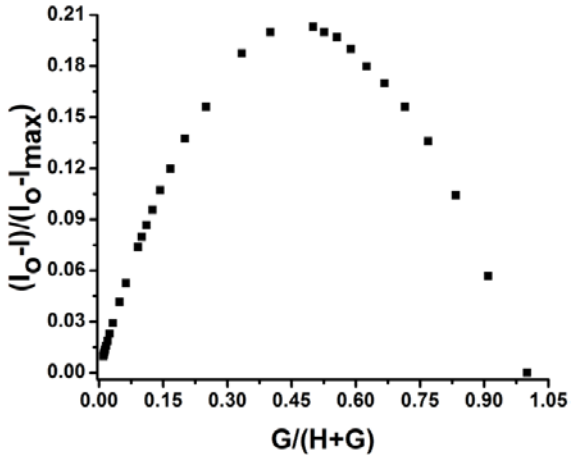

Figure S39. Assessment of the stoichometry of the AMP complex of **1** via Job plot analysis; [**1**] + [AMP] = 10 μM, pH 7.4 (0.01 M HEPES buffer), 25^{o}C.

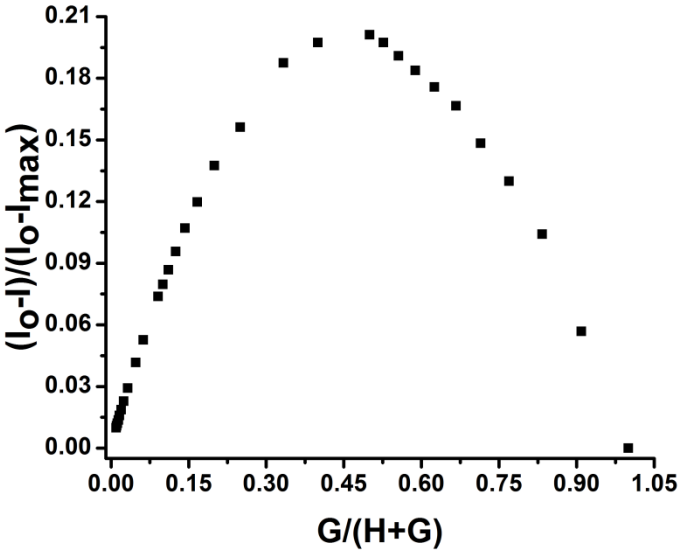

Figure S40. Assessment of the stoichometry of the ADP complex of **1** via Job plot analysis; [**1**] + [ADP] = 10 μM, pH 7.4 (0.01 M HEPES buffer), 25^{o}C.

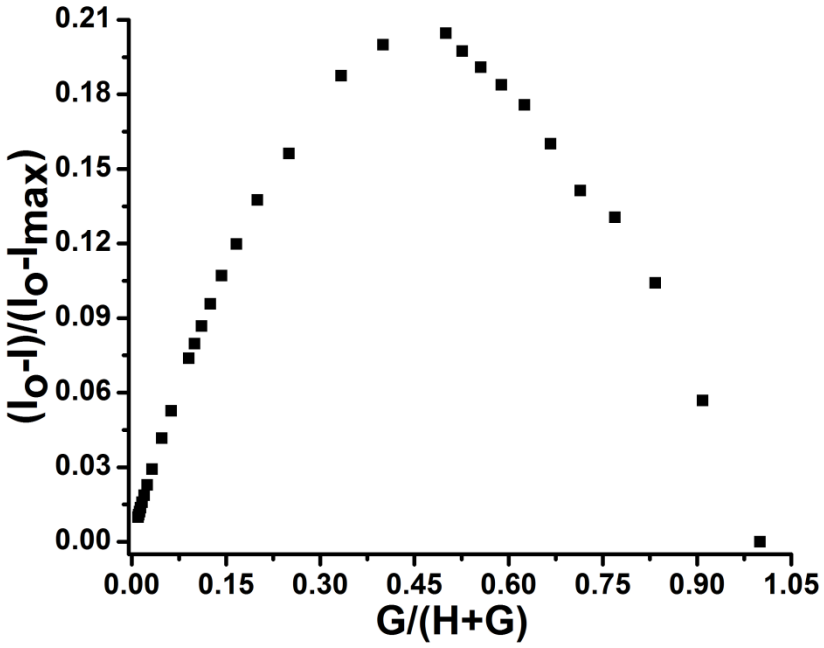

Figure S41. Assessment of the stoichometry of the ATP complex of **1** via Job plot analysis; [**1**] + [ATP] = 10 μM, pH 7.4 (0.01 M HEPES buffer), 25°C.

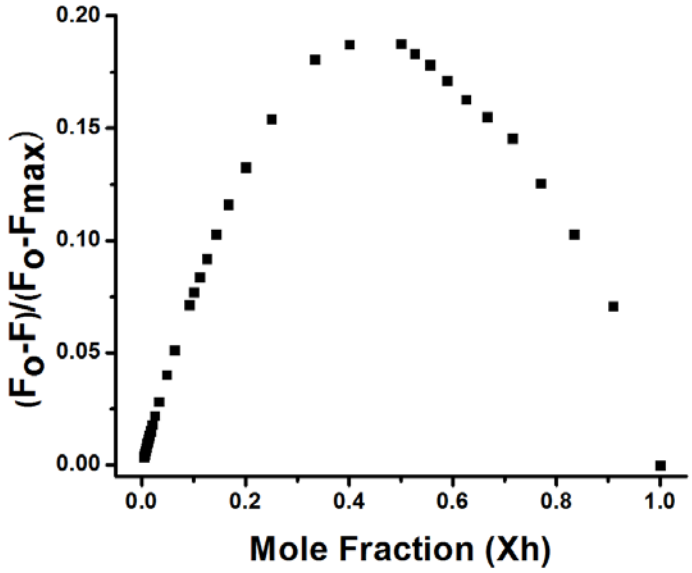

Figure S42. Assessment of the stoichometry of the GTP complex of **2** via Job plot analysis; [**2**] + [GTP] = 10 μM, pH 7.4 (10 mM HEPES buffer), 25°C.

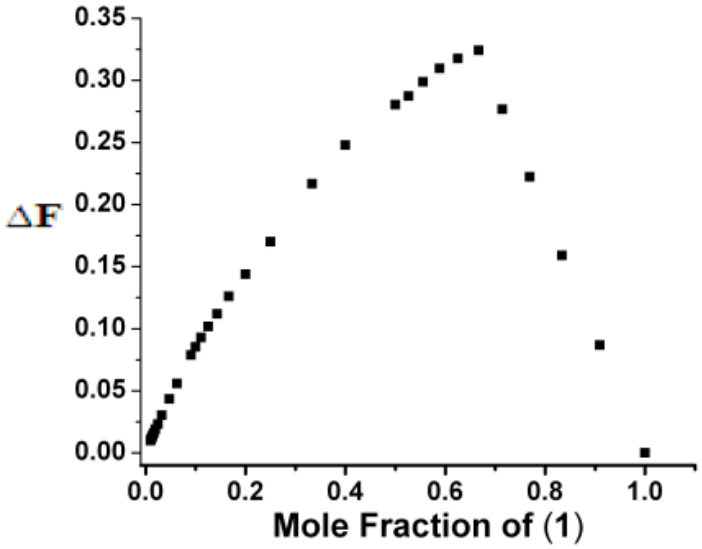

Figure S43. Assessment of the stoichometry of the PPi complex of **3** via Job plot analysis; [**3**] + [PPi] = 10 μM, pH 7.4 (10 mM HEPES buffer), 25ºC.

UV/vis Analysis:

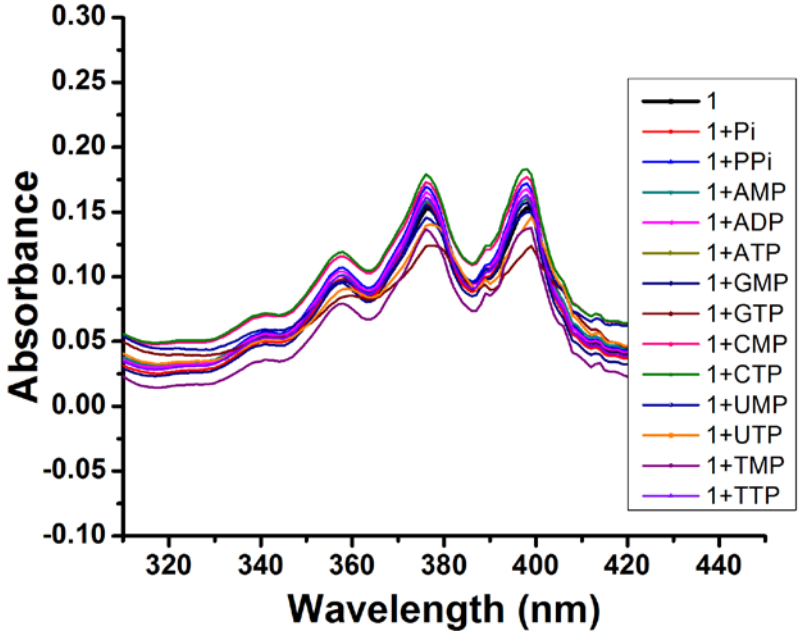

Figure S44. Absorption spectra of **1** (10 μM) upon addition of n-tetrabutyl ammonium salt of Pi and PPi and sodium salts AMP, ADP, ATP, GMP, GTP, CMP, CTP, TMP, TTP, UMP and UTP, (10 equiv) at pH 7.4 (0.1M HEPES buffer, 25^{o}C).

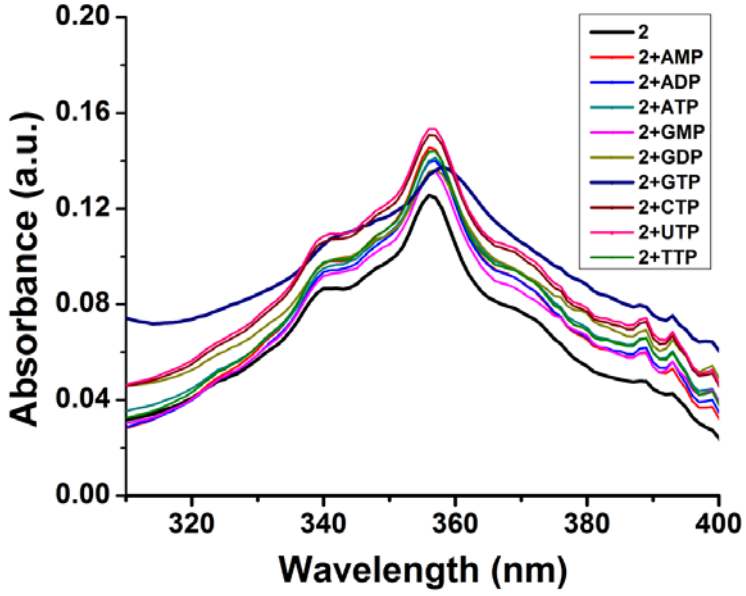

Figure S45. Absorption spectra of **2** (10 μM) upon addition of sodium salts AMP, ADP, ATP, GMP, GDP, GTP, CTP, TTP and UTP, (10 equiv) at pH 7.4 (10 mM HEPES buffer, 25ºC).

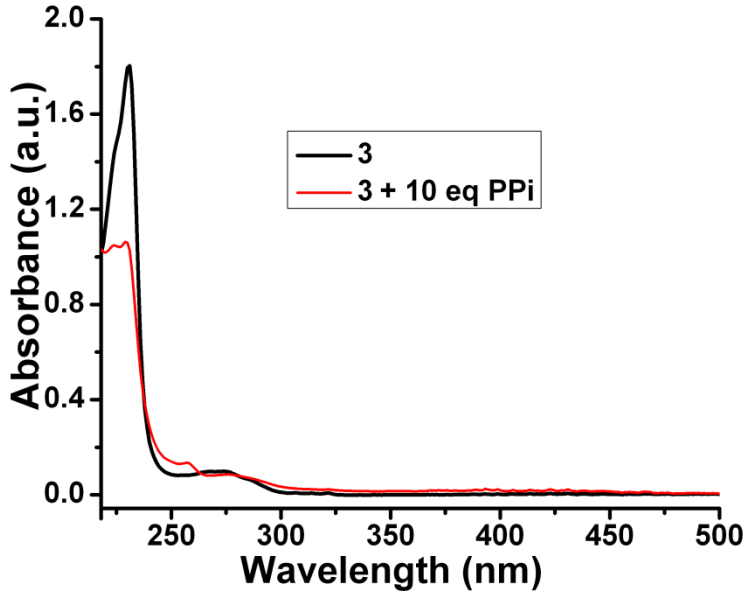

Figure S46. UV/vis change of **3** (10 μM) upon addition of 10 equiv of PPi in HEPES buffer (10 mM, pH 7.4).

Table S1: Results of Binding Stoichiometries, Binding Constants and Detection Limits of Probes **1**, **2**, and **3** with Selected anions.[a]

probe	anion	binding stoichiometry	binding constant (M^{-1})[23]	detection limit[24] (M)
1	AMP	1:1 (Figure S39)	$(7.8\pm0.2) \times 10^4$ (Figure S22)	1.26×10^{-6} (Figure S27)
	ADP	1:1 (Figure S40)	$(1.93\pm0.09) \times 10^3$ (Figure S23)	1.32×10^{-6} (Figure S28)
	ATP	1:1 (Figure S41)	$(1.8\pm0.08) \times 10^3$ (Figure S24)	1.34×10^{-6} (Figure S29)
2	GTP	1:1 (Figure S42)	$(1.1\pm0.07) \times 10^3$ (Figure S33)	6.1×10^{-7} (Figure S34)
3	PPi	2:1 (Figure S43)	$(2\pm0.1) \times 10^5$ $(1.2\pm0.01) \times 10^7$ (Figure S36)	2.42×10^{-8} (Figure S38)

[a]Anions are selected from selective fluorogenic sensing results.

Quantum Yield Measurements

Absolute fluorescence quantum yields for **1**, **2** and **3** were measured using Shanghi 756 MC UV-Vis spectrometer and Shimadzu RF-5301 PC spectrofluorophotometer. Anthracene as standard was used for quantum yield measurement of probes **1** and **2** while naphthalene standard was used for quantum yield measurement of probe **3**. Typically, the quantum yield was obtained by integrating the photons emitted by **1** up to 600 nm and calculated according to following formula. [2]

$$\Phi_{(Un)} = [FLI_{(Un)}/Abs_{(Un)}]x[Abs_{(Std)}/FLI_{(Std)}]x[\{n_{(Un)}/n_{(Std)}\}^2]x\Phi_{(Std)}$$

Where:

$\Phi_{(Un)}$ = Quantun yield of unknown

$\Phi_{(Std)}$ = Quantum yield of standard

$FLI_{(Un)}$ = Fluorescence of unknown

$FLI_{(Std)}$ = Fluorescence of standard

$Abs_{(Un)}$ = Absorbance of unknown

$Abs_{(Std)}$ = Absorbance of standard

$n_{(Un)}$ = Refractive index of solvent in which fluorescence and absorbance of unknown sample has been carried out.

$n_{(Std)}$ = Refractive index of solvent in which fluorescence and absorbance of standard sample has been carried out.

Theoretical Calculations:

Density functional theory calculation was used with the resolution of identity approximation (RI-DFT). We applied Grimme's B97-D functional[3] and TZVPP basis set[4] along with dispersion correction scheme of D3(B97-D3/TZVPP level of theory). The gas phase geometry optimization calculations were performed for probes **1**, **2** and **3** with four bromides as counter anions. Further aqueous phase calculations were conducted using the conductor-like screening model (COSMO)[5] at the previously optimized geometries. Based on the calculation results, we obtained binding modes of **1**-AMP, **2**-GTP and **3**-PPi at the same level of theory except for **2**-GTP. All calculations were performed using Turbomole 6.4 program.[6]

The energies and structures of **1** are shown in Table S2 and Figure S47. The most stable conformer of **1** has all the imidazolium moieties, with the acidic hydrogen atoms, pointing in the same direction creating an environment with strong electron affinity. The benzene moieties are anti to each other and the anthracene moieties are stacked at a distance of ~3.6 Å giving rise to an excimer.[7] This structure was chosen to study the binding mode with AMP (Figure S47). In the binding mode of **1**-AMP, the H2 and $-NH_2$ of the adenine moieties of AMP interacts with the anthracene moieties of probe **1** at distance of ~2.7 and ~2.8 Å via H-π interaction, respectively.[7] The adenine interacts with the benzene ring of cyclophane via *π-π* interaction at a distance of 3.2 Å, while the H8 of the adenine is in the vicinity of benzene at 3.3 Å. The phosphate group of AMP shows strong interactions with imidazolium protons $(C-H)^+$, forming ionic hydrogen bonds at distances of ~1.8–2.3 Å (Figure S48).

Table S2. Relative energies (kcal/mol) of **1**-4Br with respect to the most stable structure.

Complex	E^{gas}	E^{sol}
(a)	0.00	0.00
(b)	5.47	2.00
(c)	7.73	2.52
(d)	8.70	3.20
(e)	9.91	4.48
(f)	12.73	7.53
(g)	16.85	8.45

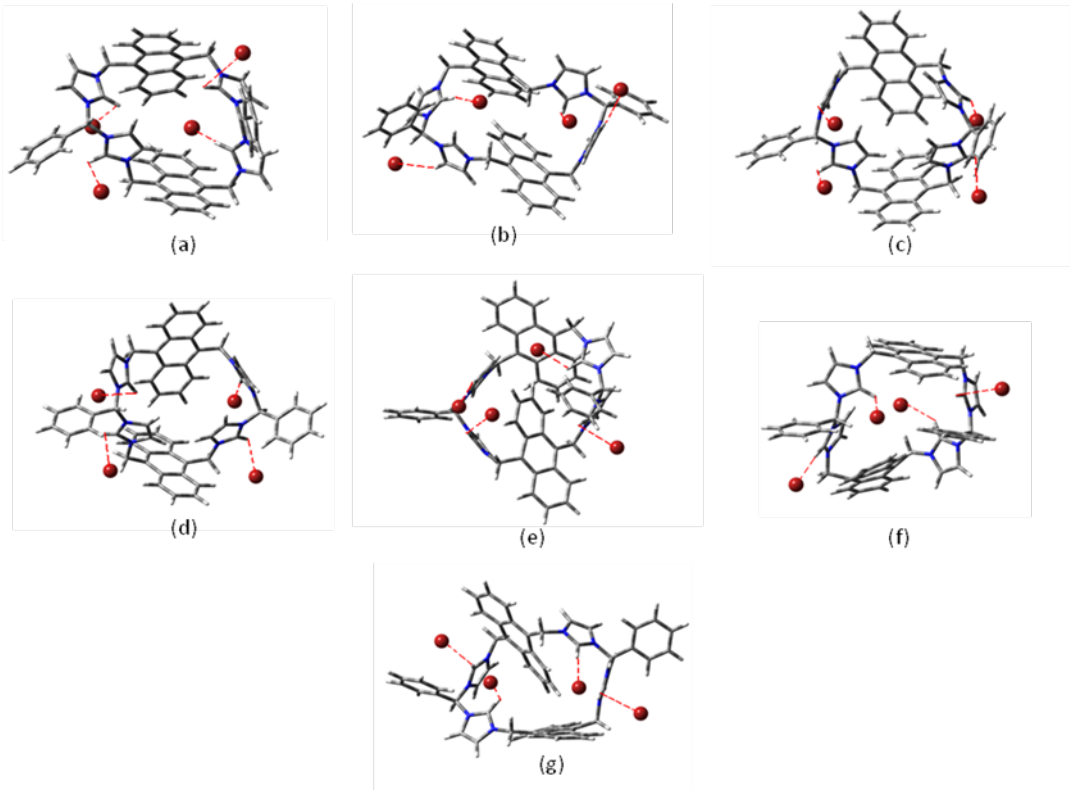

Figure S47: Stable minimum energy structures (a-f) of cyclophane **1**. Structure **a** is the global minimum energy conformer.

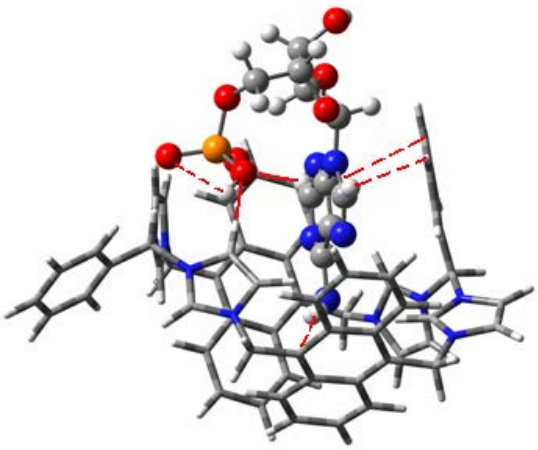

Figure S48: Optimized structure of **1**-AMP calculated at the B97-D3/TZVPP level. The adenine group is inside the cavity. Interactions of H2, H8 and amino group with fluorophores and interactions of phosphate group with imidazolium moieties can be seen with red dotted lines. Br^- counteranions are removed for the sake of clarity.

In the case of probe **2**, the energies of the low-lying structures of **2**-4Br are summarized in Table S3 and the corresponding geometries and the binding modes of **2**-GTP/GDP are shown in Figure S49. In both phases geometry (a) shows the lowest energy in which two Br^- anions are located beside **2** and other two Br^- anions are situated above and below **2**, respectively. This structure in the lowest energy was selected to conduct further calculations of **2** with GTP or GDP. For the calculation of **2**-GDP several water molecules were added to stabilize the negative charges on the diphosphate moiety.[8] But in the case of **2**-GTP, it was difficult to stabilize the entire structure only with the small number of water molecules. We employed, therefore, another method, density functional based tight binding method; to obtain the binding mode.[9] We added almost 40 water molecules to include the explicit solvent effect of water. In the binding mode of **2**-GTP (Figure S49 (g)), the ionic interaction distances between the imidazolium of **2** and phosphate moiety in GTP ($(C\text{-}H)^+\text{-}O^-$) are ~2.8 Å. On the other hand, the $(C\text{-}H)^+\text{-}O^-$ distances are 1.9 – 2.9 Å in **2**-GDP (Figures S49 (h)). Furthermore, the **2**-GTP shows stronger H-π interaction between $-NH_2$ of GTP and anthracene moiety of **2**; the distance between H(N) and anthracene is ~2.7 (~3.0) Å in **2**-GTP, whereas the corresponding distances are ~3.27 (~3.71) Å in **2**-GDP. The proximity of GTP over GDP and GMP seems responsible for the more intensive quenching in **2**-GTP case.

Table S3. Relative energies (kcal/mol) of **2**-4Br with respect to the most stable structure in the gas (E^{gas}) and aqueous (E^{sol}) phases.

Complex	E^{gas}	E^{sol}
(a)	0.00	0.00
(b)	5.18	2.12
(c)	2.90	2.19
(d)	5.62	3.36
(e)	10.36	6.53
(f)	7.59	6.54

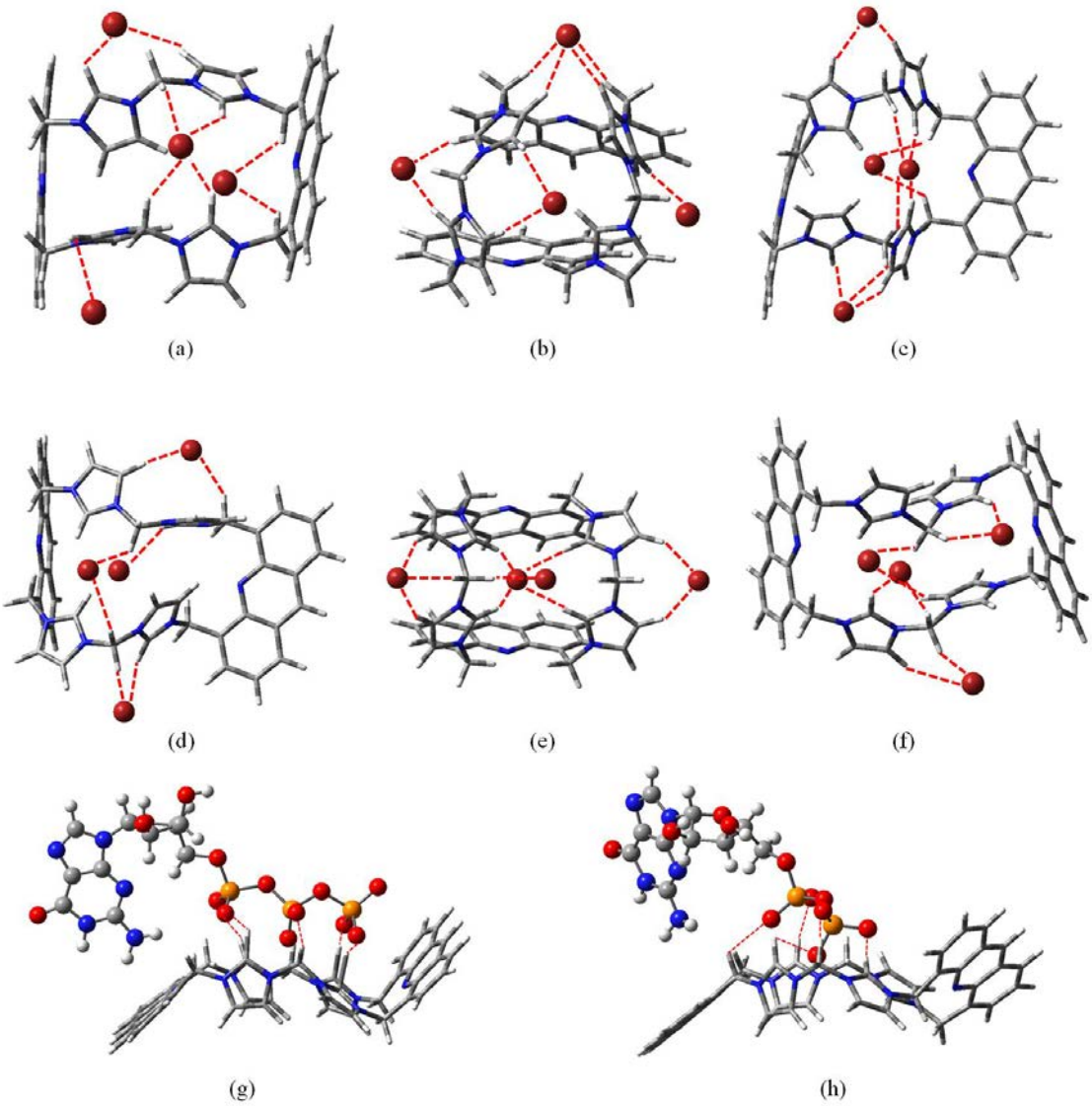

Figure S49: Optimized geometries of (a) – (f) **2**-4Br, (g) **2**-GTP and (h) **2**-GDP. Ball-and-stick represents Br^-, GTP, and GDP, while tube represents **2**. Crucial interactions are being indicated by red dotted lines. Water molecules and Br^- are deleted for (g) and (h) for clarity.

The six possible conformers of cyclophane **3** were optimized in both gas and aqueous phases. The energies and corresponding structures are presented in Table S4 and Figure S50. Among these conformers the structures (a) and (b) are nearly isoenergetic. In the most stable geometry of **3**-4Br (a), all the four Br^- anions situate outside the cavity and the imidazolium protons consequently direct inward. With reference to the NMR experimental data, structure **3** is subjected to a binding mode with PPi wherein we have witnessed the formation of an unusual dimerization of **3** with the naphthalene moieties stacked in π-π interaction. PPi molecule is aligned above the stacked naphthalenes (Figure S51). From the structure we can draw a conclusion that the electronegative environment of the PPi

draws the positively charged imidazolium moieties of **3** which is the driving force for such an alignment.

Table S4: Relative energies (kcal/mol) of low-lying energy structures optimized at B97-D3/TZVPP in both the gas and aqueous phases with respect to their corresponding global minimum energy structure.

Complex	E^{gas}	E^{sol}
(a)	0.00	0.00
(b)	0.47	0.10
(c)	6.77	1.30
(d)	2.26	1.68
(e)	4.06	2.61
(f)	4.61	3.01

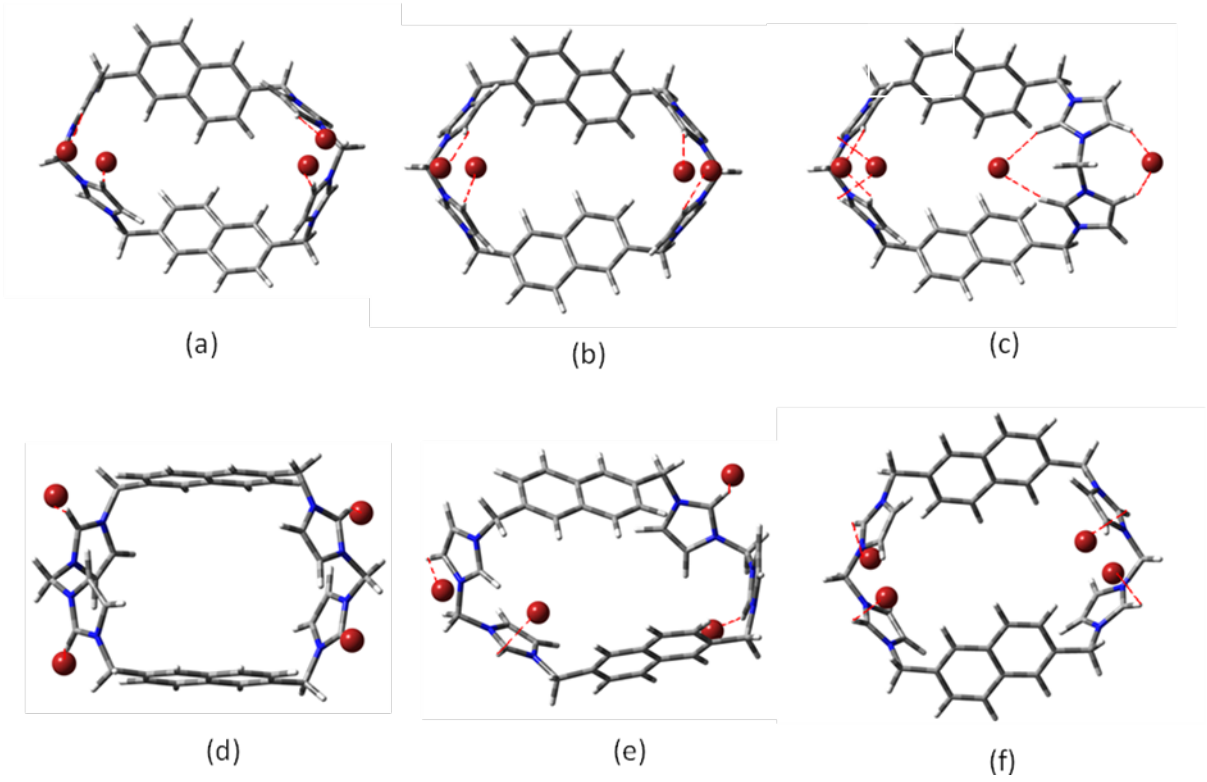

Figure S50: Stable minimum energy structures of cyclophane **3**. Structure **a** is the global minimum energy conformer.

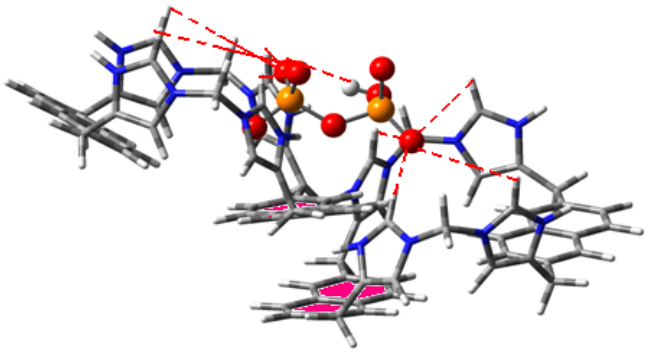

Figure S51: Optimized structure of **3**-PPi at the B97D-D3/TZVPP level. It is clearly evident from **3**-PPi complexation that the naphthalene moieties are interacting via π-stacking (highlighted in pink) at a distance of 3.07-3.59 Å. Br^- counter-anions are removed for the sake of clarity.

9. References

1. (a) Connors, K. A. *Binding Constants*: *The Measurement of Molecular Complex Stability*, Wiley, New York, **1987**. (b) OriginLab 8.0, OriginLab Corporation, Northampton, MA, **2003**. (c) Cielen, E.; Tahri, A.; Heyen, K. V.; Hoornaert, G. J.; De Schryver, F. C.; Boens, N. *J. Chem. Soc., Perkin Trans. 2* **1998**, 1573-1580.
2. Eaton, D. F. *Pure & Appl. Chem.* **1988**, *60*, 1107-1114.
3. Grimme, S. *J. Comp. Chem.* **2006**, *27*, 1787-1799.
4. Weigend, F.; Haser, M.; Patzelt, H.; Ahlrichs, R. *Chem. Phys. Lett.* **1998**, *294*, 143-152.
5. Paier, J.; Hirschl, R.; Marsman, M.; Kresse G. *J. Chem. Phys.* **2005**, *122*, 2341021-13.
6. TURBOMOLE V6.4 2012; a development of University of Karlsruhe and Forschungszentrum Karlsruhe GmbH: Karlsruhe, Germany, **2007**. Available from http://www.turbomole.com.
7. Kolaski, M.; Arunkumar, C. R.; Kim, K. S. *J. Chem. Theory Comput.* **2013**, 9, 847-856.
8. Kwon, J. Y.; Singh, N. J.; Kim, H. N.; Kim, S. K.; Kim, K. S.; Yoon J. *J. Am. Chem. Soc.* **2004**, *126*, 8892-8893.
9. (a) Aradi, B.; Hourahine, B.; Frauenheim, Th. *J. Phys. Chem. A.* **2007**, 111, 5678-5684. (b) Elstner, M.; Porezag, D.; Jungnickel, G.; Elsner, J.; Haugk, M.; Frauenheim, T.; Suhai, S.; Seifert, G. *Phys. Rev. B.* **1998**, 58, 7260-7268.